DEVELOPMENT OF NANOCOMPOSITE COATING FILM WITH GAS AND WATER VAPOR BARRIER PROPERTIES FOR BAGASSE MOLDED PULP PACKAGING

SUPATTRA KLAYYA

MASTER OF SCIENCE
IN
MATERIALS INNOVATION

SCHOOL OF SCIENCE
MAE FAH LUANG UNIVERSITY

2021

DEVELOPMENT OF NANOCOMPOSITE COATING FILM WITH GAS AND WATER VAPOR BARRIER PROPERTIES FOR BAGASSE MOLDED PULP PACKAGING

SUPATTRA KLAYYA

THIS THESIS IS A PARTIAL FULFILLMENT OF
THE REQUIREMENTS FOR THE DEGREE OF
MASTER OF SCIENCE
IN
MATERIALS INNOVATION

SCHOOL OF SCIENCE
MAE FAH LUANG UNIVERSITY
2021

DEVELOPMENT OF NANOCOMPOSITE COATING FILM WITH GAS AND WATER VAPOR BARRIER PROPERTIES FOR BAGASSE MOLDED PULP PACKAGING

SUPATTRA KLAYYA

THIS THESIS HAS BEEN APPROVED
TO BE A PARTIAL FULFILLMENT OF THE REQUIREMENTS
FOR THE DEGREE OF MASTER OF SCIENCE
IN
MATERIALS INNOVATION
2021

EXAMINATION COMMITTEE

.....CHAIRPERSON
(Assoc. Prof. Darunee Wattanasiriwech, Ph. D.)

.....ADVISOR
(Asst. Prof. Nattakan Soykeabkaew, Ph. D.)

.....CO-ADVISOR
(Asst. Prof. Nattaya Tawichai, Ph. D.)

.....CO-ADVISOR
(Asst. Prof. Uraiwan Intatha, Ph. D.)

.....EXTERNAL EXAMINER
(Assoc. Prof. Emiliano Bilotti, Ph. D.)

ACKNOWLEDGEMENTS

I am very grateful to my advisor, Asst. Prof. Dr. Nattakan Soykeabkaew for giving me the opportunity to my Master's study in Mae Fah Luang University and would like to thank for her advice and encouragement. I would also like to thanks my co-advisor, Asst. Prof. Dr. Nattaya Tawichai and Asst. Prof. Dr. Uraiwan Intatha, who always give a good advice and recommendation throughout the course. I would not have achieved this far and this thesis would not have been successfully completed without all the supports.

I am grateful to Mae Fah Luang University for supporting the grant of research publication and thesis.

In addition, I would also like to thanks the staff in Scientific and Technological Instruments Center (STIC), Mae Fah Luang University for their assistance in analysis of samples.

Finally, I most gratefully acknowledge my parent, my friends and those whose name are not mentioned here for all their supports throughout the period of this research.

Supattra Klayya

Thesis Title	Development of Nanocomposite Coating Film with Gas and Water Vapor Barrier Properties for Bagasse Molded Pulp Packaging
Author	Supattra Klayya
Degree	Master of Science (Materials Innovation)
Advisor	Asst. Prof. Nattakan Soykeabkeaw, Ph. D.
Co-Advisor	Asst. Prof. Nattaya Tawichai, Ph. D.
	Asst. Prof. Uraiwan Intatha, Ph. D.

ABSTRACT

Nowadays, the interest and awareness towards utilizing sustainable and biodegradable materials for packaging have been more realized, particularly in single use and food packaging. Molded pulp packaging from wood source and agricultural waste (e.g., sugarcane bagasse and bamboo) has gained more attention and chosen in replacement of petrochemical-based packaging. However, some insufficient performances of molded pulp packaging such as gas and water vapor barrier properties have limited its uses are limited. Nanocellulose is a promising, highly sustainable biomaterial with exceptional physicochemical properties and now drawing increasing interest for more comprehensive applications. It has unique properties, including high crystallinity, high strength, non-toxic, and outstanding gas barrier property. Thus, it has excellent potential to improve molded pulp packaging for new uses (e.g. dried food and instant food). This research aims to develop the prototype of nanocellulose integrated molded pulp packaging with enhanced gas and water vapor barrier properties sufficient to preserve dried food. In the first part, nanofibrillated cellulose (NFC) was modified by esterification reaction, which led to modified NFC (mNFC) with different degrees

of substitution (DS), between 0.21 and 0.55, as confirmed by titration, FTIR, and ^{13}C NMR. A partial fragmentation and decrease in crystallinity of mNFC were revealed by TEM and XRD. To form molded pulp sheets, 5 wt% mNFC was added into a bagasse (BG) pulp slurry, then partially dewatered before hot-pressed. mNFC worked effectively as self-retention aid, partly solving the issue of drainage during sheet forming as commonly observed from unmodified NFC. The BG/mNFC (DS 0.55) sheet exhibited an enhancement in tensile properties. Water resistance and barrier performance of the current sheets were also evidently increased. The results suggested that the higher DS on mNFC can improve water resistance and mechanical properties, simultaneously overcoming drainage challenges in processing of molded pulp products. In the second part, the molded pulp samples were surface-coated with the nanocomposite films based on modified nanocellulose (1-5% loading contents) and shellac biopolymers. An exceptional improvement in oxygen transmission rate (OTR) was obtained in a condition of BG/S-mNFC2.5; 61 cc/m^2-day, while BG/S-mNFC5 showed the lowest water vapor transmission rate (WVTR) of 8.64 g/m^2-day and water contact angle (WCA) of 87.6°. Oil resistance and mechanical properties were also positively affected by shellac coating. On the other hand, shellac gave side effects on thermal stability. The newly developed molded pulp packaging in this project were comparable to various commercial packaging materials for dried and instant food. The results indicated the high possibility in using this current pulp based integrated with nanocellulose for instant food packaging application.

Keywords: Molded Pulp, Nanofibrillated Cellulose, Shellac, Chemical Modification, Nanocomposite Coating, Water Vapor Transmission Rate, Oxygen Transmission Rate

TABLE OF CONTENTS

TABLE OF CONTENTS (continued)

LIST OF TABLES

LIST OF FIGURES

LIST OF FIGURES (continued)

LIST OF FIGURES (continued)

Figure **Page**

CHAPTER 1

INTRODUCTION

1.1 Background

Food packaging has a function to maintain the quality of food. The growth of food packaging increased over $5,052 million by 2021 [1]. Presently, dried food or instant foods are popular because of the Coronavirus disease (COVID-19) that made people stay at home. Therefore, the shelf-life of dried or instant food is essential due to the quality of packaging. These days, the dried food packaging is made chiefly from unsustainable and non-biodegradable plastic materials such as polyethylene (PE), polypropylene (PP), or polyethylene terephthalate (PET), and these materials increased waste and pollution problems worldwide (reported by the U.S. Environmental Protection Agency) [2]. Hence, pulp or paper materials have been getting more attention and chosen to replaced plastic materials. The pulp or paper produced from renewable resources such as wood or agricultural waste made them biodegradable; however, these materials are not suitable for dried or instant food [3]. The barrier properties (e.g., gas and vapor barrier) are mainly limited because pulp and paper showed many pores insides, allowing the gas or vapor molecules to pass through [4]. Consequently, the coating pulp and paper packaging is used widely to improve barrier properties [5]. Although the film could solve the barrier of pulp and paper, plastic films are not biodegradable. Therefore, it is imperative to go after the innovative materials that concern biodegradability, sustainability, and improved barrier properties.

Nanocellulose is a promising, highly sustainable biomaterial with exceptional physicochemical properties and now drawing increasing interest for wider applications [6]. This material can be obtained at a relatively low cost from renewable feedstocks,

such as wood, rendering it particularly attractive to develop sustainable barrier materials [7]. It has unique properties, including high crystallinity, high strength, non-toxic, and outstanding gas barrier property. The previous research reported that the addition of nanocellulose into paper-based materials could improve the mechanical properties and oxygen barrier of the paper board by more than 50% [8],[9]. However, the chemical structure of nanocellulose, consist of many hydroxyl functional groups, led to hydrophilic characteristics [10-13]. Therefore, the surface modification of nanocellulose was studied. Esterification, acetylation, silylation, and cabamylation are the most commonly used modification reactions. All reactions have great potentials for improving the water vapor barrier of nanocellulose depending on chemical reactants. Esterification is most common reaction to prepare greener modified nanocellulose because low toxic chemical reactant such as natural acid can be used [14].

The target to improve barrier properties of molded pulp packaging via nanocellulose integration to preserve dried or instant food while remaining environmentally friendly was aimed in this work.

1.2 Objectives

1.2.1 To modify nanocellulose by esterification reaction and to study the effect of sonication energy on degree of substitution.

1.2.2 To study the effect of integration of both unmodified nanocellulose (NFC) and modified nanocellulose (mNFC) into BG mold pulps on drainage time, mechanical and barrier properties.

1.2.3 To develop mNFC or NFC/shellac nanocomposite coating film for improving barrier of BG mold pulps.

1.3 Scope of Research

This research consists of 3 main parts: firstly, the modified nanocellulose (mNFC) was prepared and then integrated into molded pulp packaging. Nanocellulose was modified via the esterification process with a lactic acid reagent. The sonication method produced the chemical reaction at different amplitudes and times, then the degree of substitution (DS) was determined. Secondly, the unmodified and optimized DS of mNFC (1-5 wt%) were add to the bagasse (BG) molded pulp samples. Thirdly, mNFC/shellac nanocomposite was coated on BG molded pulp by casting. The preparation of a mixed solution between mNFC (filler) and shellac biopolymer (matrix) was achieved with the use of ultrasonication to enhance the dispersion. The morphology, physical, mechanical, thermal, and barrier properties of prepared BG molded pulp were studied and compared with commercial packaging materials of dried and instant food.

1.4 Molded Pulp Packaging

Nowadays, molded pulp packaging is widely used as food-related carriers, such as food containers and serving trays [15]. Molded pulp describes a three-dimensional package that has been classified in numerous ways over the years. The classification using based on the product density, production process, and fabrication method [16]. However, as per guidelines from the International Molded Fiber Association (IMFA), they can now be categorized as follows: thick wall, transfer molded, thermoformed (thin-wall), and processed [17]. This packaging produces from base materials of plant fiber pulp (e.g., wood, cotton, bamboo, sugarcane, and others) or recycles paper [18].

1.4.1 Properties of Molded Pulp Packaging

Generally, molded pulp packaging has some good properties compared with alternatives packaging [19], such as polystyrene, polypropylene, polyethylene, and polyurethane, as shown in Table 1.1.

1.4.2 Drawback of Molded Pulp Packaging

Packaging materials must have good gas barrier properties to protect the contents from exterior influences such as oxygen. The long shelf life of food affiliate with the controlling of oxygen permeable [20]. The presence of oxygen in packaged food is often a critical factor that limits shelf life. These results can cause changes in flavor, color, and odor and destroy nutrients and facilitate the growth of aerobic bacteria, molds, and insects [21]. The gas barrier properties of molded pulp packaging depend on the fiber characteristic. The micro-sized of fiber made them have many pores insides, which the molecule can transfer and reacted with food (Figure 1.1). However, the gas barrier of molded pulp packaging depends on the thickness and fiber characteristic from the pulping process, such as fiber defibrillation.

Table 1.1 The Comparison of Some Properties Between Molded Pulp and Alternative Packaging

Properties	**Molded pulp packaging**	**Alternative packaging**
Materials resource	Plant fiber (renewable resource)	Petroleum
Sustainability	Biodegradability and compostable	Non- biodegradability
Climate Tolerance	Unaffected by extreme temperature	Temperature affects brittleness
Static	Electrically neutral	Regular treatment with antistatic agent
Environment pollution	Eco friendly	Ecotoxicity, particularly microplastic in the marine environment

Source [19]

The main component of molded pulp materials is cellulose fibers that have certain hydrophilicity. Cellulose is known to have polar hydroxyl groups (–OH) that can form a strong interaction with water via hydrogen bonding (see Figure 1.2). Usually, crystalline regions in cellulose are the main part that presents strong hydroxyl groups that are not available for interaction with water because they form intra- and inter-molecular chain hydrogen bonds [22]. In contrast, the absence of structural regularity observed in the amorphous regions of cellulose increases the availability of hydroxyl groups for interaction with water molecules [23]. The previous drawback of molded pulp packaging led to the limitation for some food, especially dried food or dehydrated food.

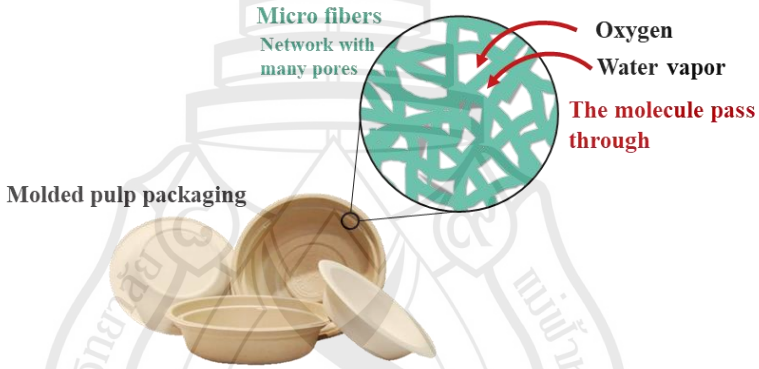

Figure 1.1 The Molded Pulp with Poor Oxygen Barrier Properties

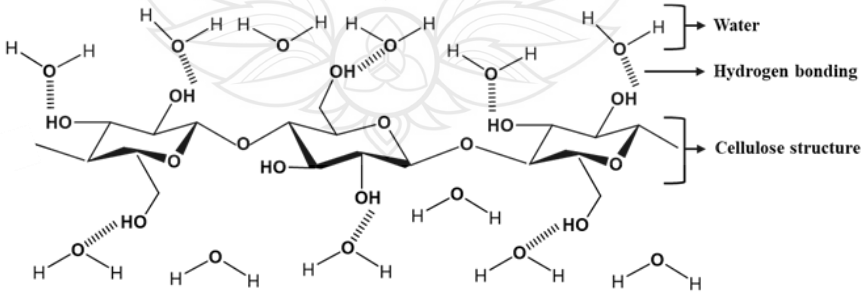

Figure 1.2 The Interaction of Water Molecules and Cellulose Structure

1.5 Dried Food Packaging

Dried food or dehydrated food including instant food products (Figure 1.3) such as noodle or soup are famous nowadays because it avoids the need for the use of refrigeration systems and reduces space requirements for storage and transport; diversify the supply of foods with different flavors and textures, thus offering the consumers a great choice when buying foods [24]. Busy lifestyles and the increased number of working populations contribute to the demand to eat dried food products [25]. The rise consumption of dried food products shows a growing trend towards the use of dried food packaging. The packaging of dried food needs to show good gas and vapor or moisture barriers and provide water resistance. Generally, dried food packaging can classify into two main types are plastic and coated or laminated packaging [26-27]

Table 1.2 Relative Value of Barrier Property for The Different Foods

Food types	**WVTR (g/m^2-day)** (80-90% RH, 20-38 ^{o}C)	**OTR (cc/m^2-day)** (0% RH, 23^{o}C)
Fresh cooking food	>15	>1550
Fresh meat (MAP)	12-80	5-200
Instant food	5-10	30-100
Dehydrated food	1.2-8	< 10
Chill food	1.5-10	< 20
Frozen	<5	<5

Source [28]

Source [29]

Figure 1.3 Dried Food and Instant Food Products

1.5.1 Plastic Packaging

Polymers or plastic packaging materials have increasingly replaced traditional materials, such as metal or glass, in many food packaging applications because of their lightweight and superior functionality [30]. The significant advantages of polymers are more flexible, various shapes, and lightweight than metal, glass, and paper. Moreover, most polymers packaging have a low cost compared to other packaging materials (see Table 1.3). Finally, polymers require less energy for manufacturing and transportation [31]. The most limiting factors for polymers as food packaging are their relatively poor barrier properties (permeability of water vapor, gases, and light) compared to metal and glass [32]. However, those barrier properties improved by laminating with aluminum foil and several different polymer films together, along with other processing technologies [33]. There are five types of polymers frequently used in food packaging: polyethylene (PE), polypropylene (PP), polystyrene (PS), polyvinyl chloride (PVC), and polyethylene terephthalate (PET or polyester) [34]. High-density polyethylene use in milk containers, detergent bottles, bags, and industrial wrapping [35]. Low-density

polyethylene (LDPE) use for film, bags, coatings, and containers. Polypropylene employ in film, crates, and microwavable containers [36]. Polystyrene finds use in jewel cases, trays, and foam insulation, while PET use in bottles, film, and other food packaging applications [37].

1.5.2 Coated or Laminated Packaging

Coating and lamination technologies have been developed rapidly over the last 40 years to meet the requirements of various food packaging applications. Coating and laminating technologies can fully utilize the advantages of each packaging material, such as metal, paper, or polymers, and combine them to create a packaging material with better barrier and mechanical properties [38]. Laminated materials are made by bonding two or more layers of webs of different packaging materials together [39]. The purpose is to create a new structure that contains the required barrier and mechanical properties (Table 1.3) [40, 41]. The most common and effective coating materials with high barriers to water vapor and oxygen are polyvinylidene chloride (PVdC) and ethylene alcohol (EVOH), but these materials have high production costs [42]. Aluminum metallization is also an effective coating to provide high barrier properties to packaging materials, mainly to provide high barrier properties against the light. The laminate of molded pulp or paper by polyethylene (PE) is widely used to contain dried food because molded pulp or paper provides stiffness, strength, shape, and heat sealing, whereas PE provides a barrier to moisture and gases [43].

However, laminated packaging are very environmentally unfriendly because it is very difficult to separate the different materials and hence limited the choices for waste handling afterwards. Therefore, to improve barrier properties of molded pulp packaging was developed using green nanotechnology such as addition of nanocellulose seem to be a better approach.

Table 1.3 Water Vapor Transmission Rate (WVTR) and Oxygen Transmission Rate (OTR) for Some Plastic Polymers Used to Package

Commercial materials food packaging	**WVTR (g/m^2-day)** (80-90% RH, 20-38 °C)	**OTR (cc/m^2-day)** (0% RH, 23°C)
Plastic packaging		
LDPE	12.5-23	1300-8500
HDPE	3.7-9	300-3100
PP	4.6-12	700-3100
OPP	3.9-6.2	420-2500
PET	39-51	21-129
EVOH	22-2500	0.08-0.19
PA	300-400	10-16
PVDC	40	115
OPA	260	18.6-39
OPS	109-170	4350-6200
PVC	40-200	30-75
PS	70-150	300-1300
Aluminum foil	0	0
Laminate packaging		
Paperboard	>500	>10000
Metal/PET	0.5	0.1
PA/PE	0.9-5	5-90
PVDC/OPP	-	4.7-9.3
Kraft paper/LDPE	4.8	0.9
PET/PE	0.2-0.4	110
Metal/OPP	0	19-160
PVDC/polyester	6	14

1.6 Nanocellulose

Nanocellulose offers a wide range of applications from basic industrial materials like foods, cosmetics, and textiles. Furthermore, they use advanced materials such as foldable electronics, high-performance nanocomposites, power devices, and reinforcement in food packaging. In food packaging, nanocellulose improves gas barrier properties, good mechanical strength, and heat resistance [44]. Nanocellulose can divide into two types depending on its pretreatment. They extract from wood and other vegetable sources, namely cellulose nanocrystals (CNCs), also called cellulose whiskers, and cellulose nanofibrils (CNFs), also called nanofibrillated cellulose or NFC (Figure 1.4) [45].

CNCs obtained by the chemical hydrolysis of the amorphous regions of cellulose and it does show rod shape of fiber length 100-600 nm with dimension 2-20 nm makes its low surface area. On the other hand, CNFs are obtained by subjecting a cellulose suspension to a mechanical process and show fiber length more than 1000 nm with dimension 5-30 nm make it has a high surface area [46]. The excellent oxygen barrier properties of nanocellulose can attribute to the dense network formed by nanofibrils with a high specific area, smaller and more uniform dimensions [47]. The dense nanofibrils form more complex and smaller pores compared to cellulose nanocrystals which are on a micro-scale.

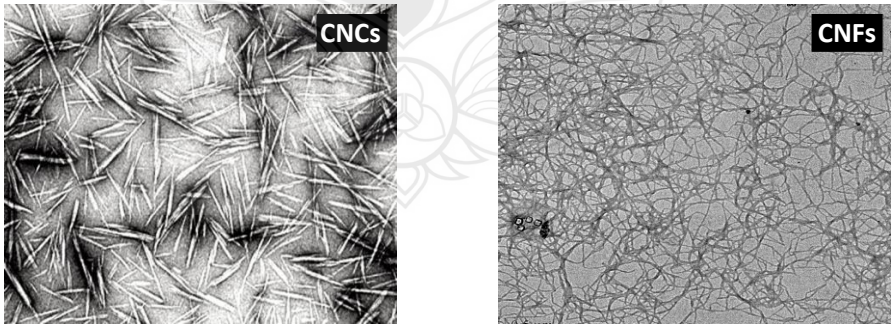

Source [45]

Figure 1.4 Cellulose Nanocrystals (Left) and Cellulose Nanofibrils (Right)

CNFs are limited to water vapor resistance because it provides a large specific surface area along with numerous free hydroxyl groups on its surface that generate vast hydrogen bond interactions between nanofibrils rendering it hydrophilic [48]. The hydrophilic behavior of cellulose affected high water molecules pass through the structure that is not suitable for barrier packaging. Different chemical modifications in earlier research have modified the hydrophilic characteristics of the CNFs.

1.7 Modification of Nanocellulose

The chemicals modification of nanocellulose is widely used in 4 main reactions that are esterification, acetylation, silylation, and cabamylation [49].

1.7.1 Esterification

Esterification is a dehydration reaction that is often not feasible in the water medium, as the reaction product itself is a water molecule. The product water is in equilibrium with medium water, and the reaction is not preferred due to the law of mass action [50].

1.7.2 Acetylation

Acetylation is a reaction between the OH-groups and acetic acid. The acetylation of cellulose depends on the accessibility and susceptibility of the OH-groups in the amorphous and crystalline regions within the cellulose polymer chain [51]. However, this reaction is not eco-friendly because the organic solvent is more toxic [52].

1.7.3 Silylation

Silylation consists of introducing substituted silyl groups on CNF surfaces. The silylation of cellulose fibers was studied, primarily to impart hydrophobic properties. Although silylation is major to improve hydrophobicity, it was limited to food packaging because of the toxicity of chemical substances [53].

1.7.4 Cabamylation

Cabamylation is a reaction that introduces an isocyanate onto the surface of cellulose [54]. However, the introduction of the toxic isocyanate and toluene decreased the “green” character of the process [55]. Toluene was used as a non-swelling solvent to avoid changing the cellulose structure and avoid reagent penetration inside the CNFs.

From Table 1.2 [56-65], all of the reactions use to modify nanocellulose for improving hydrophobicity; however, it was showed different reagents and solvents for use. Esterification reaction showed very low toxicity of reagent and solvent that safety to use in food packaging. Nanocellulose modification by reaction of acetylation, silylation, and cabamylation has been the subject of very few studies and use in food packaging applications due to the toxicity of solvent and isocyanate. Indeed, greener alternatives are available to confer similar properties. Therefore, this research will focus on modifying nanocellulose via esterification by using lactic acid to improve the barrier properties of food packaging

1.8 Biopolymer

Biopolymers are polymers produced by or derived from living organisms, such as plants and microbes, rather than from petroleum, the traditional source of polymers. The primary sources of biopolymers are renewable [66-67]. Based on their origin, three types of biopolymers can be traditionally distinguished into microbial, synthetic, and natural biopolymers [68].

1.8.1 Synthetic Biopolymer

Biomass-based such as polylactic acid (PLA) is also a crystalline polymer (37% crystallinity). It has a glass transition temperature of 60–65^{o}C and a melting temperature of approximately 175^{o}C. L-lactide (L-PLA) homopolymer is a semicrystalline polymer with high tensile strength, low elongation, and a high modulus that makes them suitable for orthopedic fixation sutures that have wild applications like load-bearing [69-70].

Table 1.4 Chemical Reactions and Strategies Used to Modify Nanocellulose

Source of cellulose	**Chemical's reaction**	**Reagent**	**Solvent**	**DS ***	**Ref**
Bacterial Cellulose	Esterification	Palmitoyl acid	Gas phase	1.47–2.01	[56]
Bleached soft wood sulfite fibers (BWS)	Esterification	Lactic acid	Water	-	[57]
Cellulose powder	Esterification	Oleic acid and Fatty acid	-	<0.3	[58]
Cellulose whisker	Acetylation	Anhydride	Organic solvent	-	[59]
Bacterial Cellulose	Acetylation	Acetic anhydride	Acetic acid + toluene	0.04–2.77	[60]
BWS	Acetylation	Acetic anhydride	Dimethyl-formamide	1.5–1	[61]
Kenaf Bast Fibers	Acetylation	Acetic anhydride	Pyridine	1.07	[62]
Sugar Beet Pulp	Silylation	Isopropyl dimethylchlorosilane	Toluene	0.025–0.36	[63]
Bleached Spruce Sulfite Cellulose	Silylation	Chlorodimethyl isopropylsilane	Toluene	0–0.16	[64]
CNFs	Cabamylation	n-octadecyl isocyanate	-	-	[65]

1.8.2 Microbial Biopolymers

Polyhydroxyalkanoates (PHA) and polyhydroxybutyrate (PHB) are the leading group of microbial biopolymers. The coating material can improve the permeability of water and oil, and at the same time, improve the packaging strength [71-72].

1.8.3 Natural Biopolymer

Protein (collagen, whey and zein), polysaccharides (pectin, starch, cellulose derivatives, carrageenan and chitosan) and lipid (beeswax and shellac) are a group of natural biopolymers. The films of protein and polysaccharides are generally good barriers against oxygen at low to intermediate relative humidity and have good mechanical properties; while lipid film promote better water vapor barrier [73].

Biopolymer films are highly available and biodegradable. However, only one type of biopolymer cannot promote overall oxygen and water vapor barrier properties. [74]. Nanofiller addition to form nanocomposite materials for enhance barrier properties is found to be one of the effective approaches.

1.9 Shellac

Shellac is natural, non-toxic, biocompatible and biodegradable polymer. It is a natural polyester resin secreted by insects *Kerria Lacca* [75]. Shellac is a natural product with interesting properties and an exceptional versatility. It is the only known commercial resin of animal origin [76].

1.9.1 Chemical Composition of Shellac

The main components of shellac are aleuritic acid, butolic acid**,** shellolic acid and jalaric acid. It was found that depending on the shellac type aleuritic acid and homologues of shellolic acid make about 70% of the total. Besides the individual acids also several esters as well as the position of the ester linkages have been identified (Figure 1.5) [77].

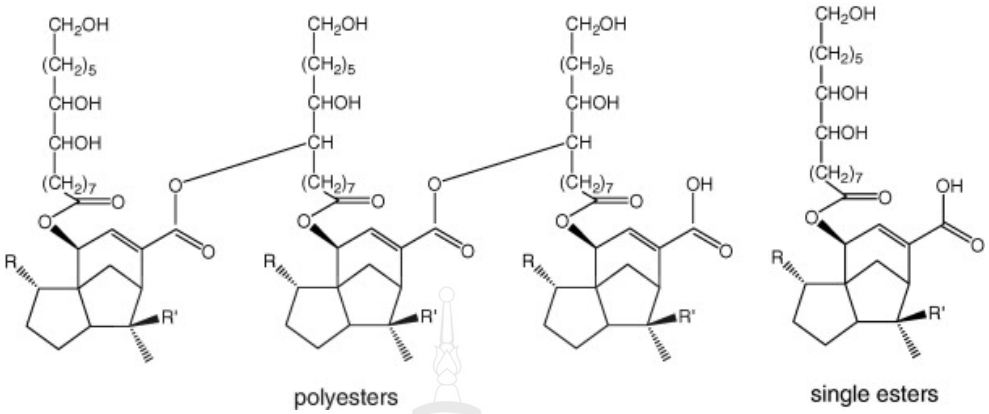

Source [78]

Figure 1.5 Chemical Structure of Shellac

1.9.2 Properties of Shellac

Shellac is a hard, brittle and resinous solid. It is practically odorless in the cold but evolves a characteristic smell on heating and melting. Its color is dependent on the type of seedlac and the refining process and can range from pale yellow to deep red (Figure 1.6). Shellac films provide high gloss, a low permeability for water vapor and gases and good dielectric behavior. Shellac is water insoluble but it is soluble in ethanol, methanol and partially soluble in ether, ethyl acetate and chloroform [79].

Source [80]

Figure 1.6 Shellac with Different Colors

1.9.3 Application of Shellac

Shellac is listed as GRAS (generally recognized as safe) by the FDA (food and drug administration). This regulatory status allows its use as additive in food products which is the most common application of shellac. Shellac is used as coating material on confectionaries and fruits to apply gloss [81]. Moreover, the application of shellac as matrix material in so-called biocomposites for the production of biodegradable composite materials may also be of interest as well as the application in paper-based packaging materials to improve water resistance.

1.10 Nanocomposite

Nanocomposite is a new generation of packaging materials with a combination of bio-based polymer and fillers that have at least one nanometer scale dimension. In nanocomposite films, the biopolymer acts as a matrix, while the nanofillers are dispersed there to improve the functional properties [82]. Nanocomposites have a set of improved properties, such as mechanical, oxygen barrier, or physical properties [83]. A nanocomposite consists of a multiphase material derived from the combination of two or more components, including a matrix (continuous phase) and a filler (discontinuous phase) at the nanometer scale (nano dimensional phase, i.e., nanostructure), were both obtained from fully renewable materials [84-85]. In this work, a matrix phase is biopolymers and a filler phase are cellulose nanofibers (Figure 1.7). The cellulose nanofibers phases have a structural role, acting as reinforcements for improvement of mechanical, barrier and physicochemical properties of the biopolymer matrix by promoting the stress transfer across the interface established between them [86]. In particular, they are promising in providing excellent barrier properties, because it is expected that the presence of these reinforcement layers will be able to delay the molecule pathway, making the diffusive path more tortuous.

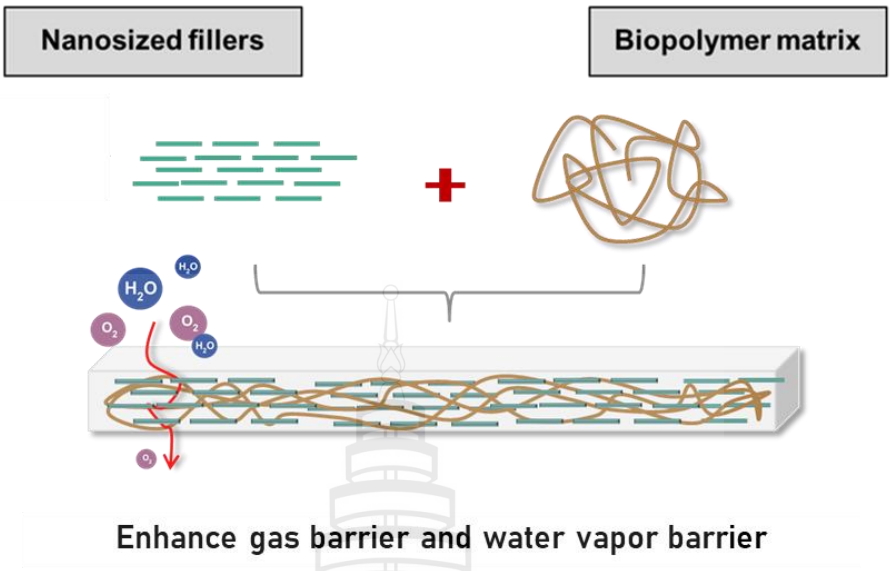

Source [87-88]

Figure 1.7 Nanocellulose-Based Composite Films from Modified Cellulose Nanofibers and Various Biopolymers with Their Functional Properties

CHAPTER 2

LITERATURE REVIEWS

2.1 Nanocellulose Integration in Pulp and Papers

Several papers published the effect of nanocellulose on paper properties. Eriksen et al. added 4wt% of nanocellulose into laboratory TMP hand sheets. They promoted increased air resistance and increase in tensile strength to 21% [89]. Taipale added 5wt% of nanocellulose to hand sheets. They presented a strong increase in Scott Bond (up to 55%) and a good increase in the tensile index (up to 15 Nm/g) [90]. Taipale and Manninen added 5% of refined nanocellulose to chemical pulp hand sheets. They saw comparative expansions in rigidity to those seen by not really settled that nanocellulose expanded the extension coefficient of uninhibitedly evaporated sheets by 30% [91]. Similarly, Heijnesson-Hulten used TEMPO-oxidized nanocellulose in laboratory CTMP hand sheets. With addition levels at 5%, there was an improve in mechanical strength by almost 200% (from 137 kPa to 387 kPa) [92-93]. The TI (tensile index) improved noticeably at 20% (at 8 Nm/g), as with the pulps process in the Taipale and Manninen studies.

The previous review showed the principal function of nanocellulose by improving mechanical properties with a 1-5% range of loading contents, while the side affected of dewatering and low water resistance, poor barrier properties were reported in many researches. The reduction made by additive using or modification method. However, the commercials scale wants to avoid using additives because it increased cost production, including non-recovery. So, the modified nanocellulose would be a good target way.

Sethi et al. studied modified nanocellulose (mNC) on water removal in the paper-making process. The mNC produced by the esterification reaction made them changed surface functional from hydroxyl to the ester group. The results modified NC

helped reduce the time for drainage water (from 45 min to 10 min). Moreover, the 10% loading contents of mNC in the paper sheet have improved the modulus and strength of the paper [94]. Lu et al modified MFC by using coupling agents. The surface of modified MFC changed the character from hydrophilic to hydrophobic. Moreover, the crystallinity of the cellulose remained intact. The titanate modifier showed lower polarity that made it most hydrophobic surface among the tested coupling agents to yield [95].

Bras et al. studied the water vapor permeability of film made from cellulose-esters, and the resulting films found practical barriers to water vapor transport [96]. Saha et al. prepared a nanocomposite film by using cellulose acetate as filler [97]. These cellulose acetate-based nanocomposites could an active packaging material due to their excellent antimicrobial activity and non-toxicity. According to the above literature review, this research project wanted to optimize quantities for add modified nanocellulose to increase the ability to block the permeability of oxygen and moisture to the paper packaging using green modification methods like esterification.

2.2 Bio-Nanocomposite Coating Film with Nanocellulose

The nanocomposite coating shows outstanding mechanical and barrier properties. Many researchers have widely used biopolymer matrix from thermoplastic corn starch (TPCS), starch (ST), chitosan (CH), polylactic acid (PLA), whey protein (WH), alginate, gelatin (G), cellulose, and shellac (S) to improve some properties of packaging. Martins et al. prepared TPS composites via using glycerol as plasticizer and bacteria cellulose (1-5 %, w/w) as a filler agent. The bacteria cellulose dispersed well in the matrix, and there is a strong adhesion between bacteria cellulose and TPS. At 5 % BC loading, modulus and strength of the composite were elevated considerably because there are probably due to the high aspect ratio and three-dimensional network of the BC. Generally, these materials are promising in applications of food packaging and biodegradable materials; however, TPS-based materials are sensitive to humidity. The incorporation of BC slightly reduced the moisture sorption maximum. The interpretation is that starch is more hydrophilic than cellulose and nanofibers.

Fernandes et al. prepared nanocomposite films based on chitin or chitosan (CH) and BC or NFC. The goal is to improve mechanical properties of CH films while keeping their transparency and thermal stability. Moreover, CH solutions are an efficient media for stable suspensions of NFC or BC made the components are perfectly compatible. The result demonstrates that the films are highly transparent and flexible. The nanocomposite films show excellent Young's modulus (320 % improvement, tensile strength, and thermal stability compared with control CH films. Moreover, CH and BC-based nanocomposite used successfully as the surface coating improved the printing quality of paper [98]. Kritchenkov et al. interest in nanocomposite based on CH and nanoparticles (NPs). The nanocomposite solution was prepared by a varied dosage of NPs (0.05-1% loading based on the dried weight of CH). The results showed that the condition of 0.2% NPs loading has a high oxygen and water vapor barriers, improving by 196% and157%, respectively [99]. However, this composition affected the thermal stability of film; TGA results presented residual weight at 600 ◦C (R600) decrease with increased NPs contents.

Wu et al. (2019) presented that the silver nano filler in the polysaccharide matrix improved the barrier properties of films. Silver nano filled the interspaces of the matrix and blocked the transfer of O_2 through the film [100]. These could be explained from nanocellulose also causes the reduction of oxygen permeability (OP) of the film, which contributes to forming a dense network structure of the film matrix. The diffusion path via nanocellulose reduced the OP values which promote the quality of packed food products vapor barrier [101-102].

Nanocomposites based on PLA matrix and bacteria cellulose filler (BC) were described by Tom é et al., who prepared the nanocomposite film by simple melting-mixing of BC and PLA. The hydrophobicity of BC was increased by acetylation. Therefore, their compatibility and adhesion with the PLA matrix were improved. The nanocomposites have considerably increase in Young's modulus and tensile strength by 40% and 25%, respectively due to the level of nanofiller loadings [78]. The integration of both unmodified and acetylated BC nanofibers in the PLA matrix also resulted in a considerable increase thermal properties which observed by the increment in both initial and maximum degradation temperatures. Song et al. (2014) studied on the feasibility

of integrating modified NFC in the PLA matrix improves the water vapor barrier of the film [103].

Shankar et al. observed that the alginate film was improved vapor barrier from an increased tortuous path of nanotubes and AgNPs [104]. However, the critical concentration of nanofillers would be increase the vapor barrier of nanocomposite films. Zahedi and co-authors established that modified nano-clay effectively reduces the WVP of carboxymethyl cellulose films than unmodified nano-clay. These differences may result from various structural and arrangement features. Nanoclays impede water vapor diffusion because of the impermeable layers of this type of nanofiller [105]. The presence of hydrophilic Si-OH groups can affect the hydrophilicity of the film surface. The addition of nanoparticles (CMC) to gelatin coatings increased the vapor permeability value of the film attribute to the hydrophilic nature of CMC [106].

The research team of Maduka L. developed the coating solution for wood surface from shellac-based nanocomposite [107]. The different unmodified and modified nanoparticles (1-3%) were dispersed in shellac solution. The results show that modified nanoparticles can improve the hydrophobic behavior of the shellac at a reasonable level compared with unmodified nanoparticles. Another review about nanocomposite from various biopolymers was summarized in Table 2.1. The information expected that most of the biopolymer matrix from polysaccharide sources shows the prominent property of resistance to air permeability and can improve the mechanical properties of substrate in some cases. Polyester matrix gives the outstanding property of low water vapor transmission. Especially when filled with nanocellulose, it showed both low water and gas permeable. Therefore, this study will focus on nanocomposite film by using shellac as a matrix phase because solvent has low toxicity.

Table 2.1 Properties of Nanocomposite Films Based on Nanocellulose and Biopolymers

Matrix	Solvent	Filler	Properties	Ref.
PHB	Chloroform	CNC	Improve gas barrier and migration properties	[108]
PLA	Ethyl acetate	mNFC	Low WVTR	[109]
PLA	Ethyl acetate	CNC	Improve mechanical and antimicrobial	[110]
ST	Chloroform	CNF	CNF increased inhibition effect toward gram-positive	[111]
CH	Acetic acid	CNF	Improve mechanical and transparency	[112]
ST	LiCl	CNC	Improve the mechanical and the resistance to air permeability	[113]
WH	Water, Ethanol	TiO_2 nanoparticle	OTR of why protein film <1.0 and modulus increase to 100% when add 1%wt of TiO_2	[114]
ST	Acetic acid	Chitin nanofiber	High water absorption	[115]
G	Acetic acid	Nanoclay (MMT)	Improve tensile strength of the films	[116]
ST&G	Chloroform	ZnO nanorod	Low OP, increase in mechanical and heal seal properties of the films.	[117]
PLA	Dichloromethane	Modified nanofibers	Decrease in water vapor permeability	[118]
S	Ethanol	Microfibrillar cellulose	Low oxygen transmission rate and the water vapour transmission rate	[119]
S	Ethanol	Nanoparticles	Contact angle of film shows hydrophobic properties (≈78-100°)	[120]

Note PHB: polyhydroxybutyrate, PLA: polylactic acid, ST: starch, CH: shitosan, WH: whey protein, G: gelatin, S: shellac.

CHAPTER 3

METHODOLOGY

3.1 Molded Pulp Integrated with Modified Nanofibrillated Cellulose (mNFC)

3.1.1 Materials

The bleached bagasse (BG) paper was kindly supplied by Biodegradable Packaging for Environment Public Co., Ltd., Thailand. Cationic polyacrylamide (CPAM) was supported by Welkin Enterprise, Thailand. Nanofibrillated cellulose (NFC) prepared from bleached softwood was purchased from Cellulose Lab Co., Canada. L-(+)-Lactic acid (LA) (80%w/v) was purchased from Union Science, Thailand.

3.1.2 Preparation of Modified Nanofibrillated Cellulose (mNFC) with Different Degree of Substitution (DS)

The NFC stock solution was prepared to 0.4wt% suspension and then 4.4wt% LA loading content (according to the unmodified NFC dry content) was added. The suspension (~ 50 ml) was stirred at 400 rpm for 5 min using a homogenizer and sonicated with a 750 W and 20 kHz ultrasonic probe (VCX750, Sonics Materials Inc., USA) with a probe diameter of 13 mm at different amplitude percentages (30%, 50%, 70% and 90%) and time (10 to 60 min) for the anticipating different DS from varied ultrasonication energy input [121]. Then, all suspensions were kept in the oven at 100 °C for 36 h, detailed steps can be found in Sethi et al., 2017, 2018. The obtained mNFCs at different amplitudes (mNFC30, mNFC50, mNFC70, and mNFC90) were characterized and analyzed in terms of the DS, structure, and morphology.

3.1.3 Preparation of Molded Sheets, NFCs and mNFCs Integrated Molded Sheets

BG pulp was used as a base material to prepare molded sheet samples. The small pieces of BG paper were soaked in tap water overnight, and then defibrillated into a pulp slurry by using a kitchen blender (House Worth, HW-BDC2PC) at the speed of 15,000 rpm for 5 min. After that, the unmodified NFC or mNFC solution with 5wt% loading content (according to the dry BG pulp weight) was added to the BG slurry (2% pulp consistency). Then, the BG/NFC and BG/mNFC mixtures were blended at the speed of 450 rpm for another minute before pouring each mixture into a circle mold (diameter of 16 cm) with metal meshes (no.400) to partially dewater and preform the sheet. Next, the mold set was hot-pressed at 130ºC under the pressure of 159 kPa for 5 min. The system of BG/NFC sheet with addition of a typical retention aid additive CPAM was also prepared for comparison. The 0.05wt% CPAM solution was added into the BG/NFC slurry at the loading content of 0.15wt% based on the dry BG pulp weight, then preformed and hot-pressed to obtain the BG/NFC+CPAM sheet. This CPAM loading content was chosen based on previous works [122-123] that showed high dewatering efficiency of more than 50% during sheet forming. A blank (or pure) BG sheet without addition of neither NFC nor CPAM was also made for comparison, following the same procedure. All molded sheets prepared were aimed to be about 350 g/m^2 and their sample codes and compositions were summarized in Table 3.1.

Table 3.1 The Sample Code and Composition of All Molded Sheets Prepared in This Study

Sample code	Conc. BG suspension (%w/w)	NFC loading contents (%)	mNFC loading contents (%)	CPAM loading contents (%)
BG	2	-	-	-
BG/NFC	2	5	-	-
BG/mNFC30	2	-	5	-
BG/mNFC90	2	-	5	-
BG/NFC+CPAM	2	5	-	0.15

3.2 Molded Pulp Coated Nanocomposite Film of Modified Nanofibrillated Cellulose (mNFC) and Shellac

3.2.1 Materials

The base paper from bagasse (BG) was kindly provided by Biodegradable Packaging for Environment Public (Thailand). The food-grade shellac (S) was supported by Shellac Thailand. Nanofibrillated cellulose (NFC) was purchased from Cellulose Lab (Canada), and this NFC was modified by esterification reaction to generate modified nanofibrillated cellulose (NFC). Polyethylene glycol with low molecular weight was obtained from Chemipan (Thailand), while 95% ethyl alcohol was supplied by UP Marketing General Supply (Thailand).

3.2.2 Preparation of Shellac and Shellac-Based Nanocomposite Solutions

Shellac solution was prepared by 12 wt% shellacs dissolved in ethanol 95%, while shellac-based nanocomposite was prepared from mixing 12 wt% shellac solution with 1-5% loading content of NFC or mNFC before homogenization for 5 min. Then, all shellac-base nanocomposite solution was degassed and bubbles by using ultrasound energy from sonication for 10 min which the PEG was used as a plasticizer with a concentration of 10wt% to improve shellac stability in all conditions.

3.2.3 Coating of Nanocomposite Film on Molded Pulp Surface

All bagasse (BG) sheet sample was prepared with control grammage and thickness to 350±5 g/m^2 and 300±10 μm, respectively. The first coting condition of bagasse/shellac (BG/S) was done by shellac solution from the last part, in which the solution was coated by casting technique at 40 ^{o}C for 30 min. Similar to bagasse/shellac-base nanocomposite coating, the shellac-based nanocomposite from NFC or mNFC with 1 and 5% loading contents was applied on the BG sheet the code of was showed by BG/S-NFC1, BG/S-NFC5, BG/S-mNFC1, and BG/S-mNFC5, respectively. To better explain the coating method, Figure 3.1 was presented

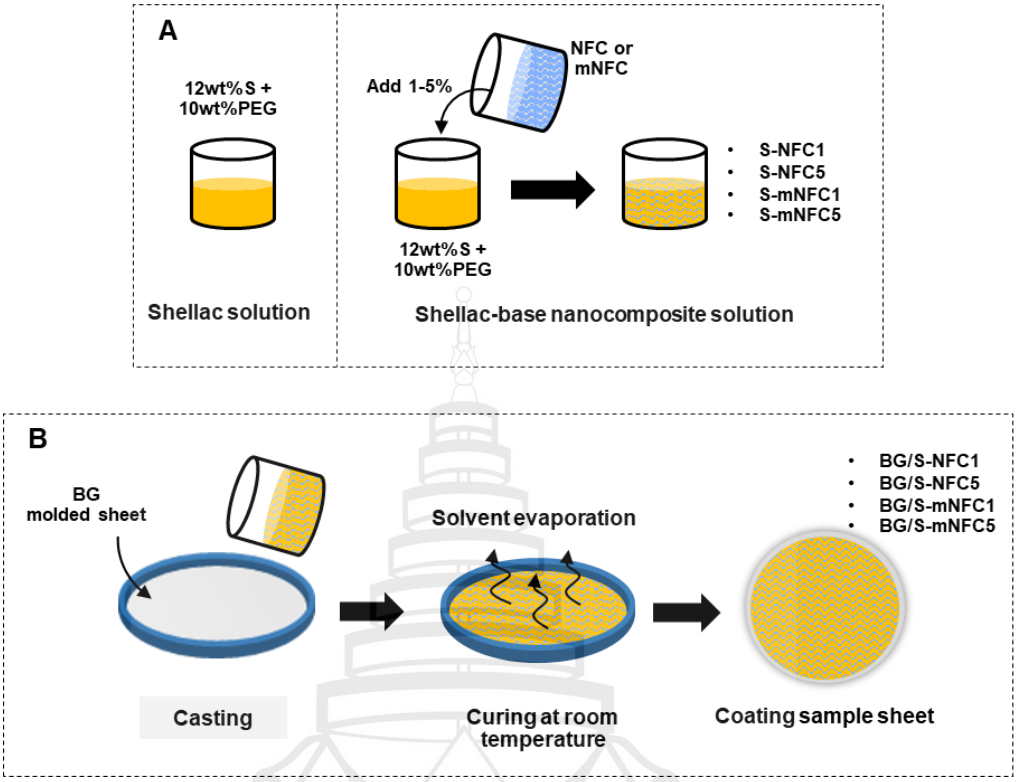

Figure 3.1 Illustration Methodology of Shellac and Shellac-Based Nanocomposite (A) Solution Preparation and (B) Coating Sample Sheet Preparation

3.3 Characterization and Testing

3.3.1 Fourier-Transform Infrared Spectroscopy (FTIR)

About 2 mg of each NFC and mNFC solid sample was manually ground with KBr powder (a ratio of 1:100) and then pressed into a circular pellet (10 mm diameter). FTIR spectroscopic analysis of the samples was performed by Perkin Elmer (Model spectrum GX, USA) with a resolution of 4 cm^{-1} and a scanning range from 500-4000 cm^{-1} [124].

3.3.2 Degree of Substitution (DS) Determined by Titration

A solid sample of 0.5 g was added to 40 ml of aqueous ethanol (70%) and stirred with a magnetic bar at 400 rpm for 30 min. Stirring was continued for 48 h at 50 °C,

after addition of 20 ml of a 0.5 M NaOH solution. Afterward, the unreacted NaOH was back-titrated with a 0.5 M HCl solution and the ester content (EC) was calculated using the following equation:

$$EC\ (\%) = \frac{[\ (Va - Vb) \times N_b - (Vd - Vc) \times N_a\ ] \times Mw}{10 \times G}$$

where Va and Vb represent the volumes (ml) of a strong base (NaOH) solution added to sample and blank, respectively, Vd and Vc are the volumes (ml) of strong acid (HCl) added to sample and blank, respectively, N_b and N_a are the respective the concentration (molarity) of NaOH and HCl solutions, Mw is the molecular weight of acid reagent and G is the weight (g) of the sample. DS was then calculated by the following equation [125]:

$$DS = \frac{162 \times EC}{Mw \times 100 - EC \times (Mw - 1)}$$

where 162 is the molecular weight of anhydroglucose monomer unit.

3.3.3 Solid-State ^{13}C Nuclear Magnetic Resonance (NMR)

Solid-state ^{13}C cross polarization-magic angle spinning (CP-MAS) NMR spectra of both NFC and mNFC were recorded at room temperature on a Bruker Avance III HD/ Ascend 400 WB, USA using a MAS rate of 5 kHz, a contact time of 500 μs, at a frequency of 100.61 MHz. Samples were packed in MAS 4 mm diameter zirconia rotors and all spectra were run for 3 h [126].

3.3.4 X-Ray Diffraction (XRD)

XRD was used to determine the crystallinity of both NFC and mNFC (X'Pert Pro MPD, UK). The X-ray diffraction patterns were recorded in a 2Θ angle range of 10º to 40º at a step width of 0.02º with a scan speed of 2°/min. The crystallinity index (CI) of the samples was calculated using Segal's equation below [127-130]:

$$CI\ (\%) = \frac{I_{002} - I_{am}}{I_{002}} \times 100$$

where I_{002} is the maximum intensity of the 002 lattice diffraction at $2\Theta = 22°$ and I_{am} is the intensity of amorphous cellulose at $2\Theta = 18°$.

3.3.5 Transmission Electron Microscope (TEM)

A 0.001% suspension of both NFC and mNFC suspension in water was sonicated in a bath with power of 73 W (Crest Ultrasonics, 690HTAE, NY, USA) for 2 min, then a 2% uranyl acetate (UA) solution was added for contrast enhancement in TEM micrographs. A drop of the suspension was deposited on a copper grid with Formvar film (200 mesh – Ted Pella) and allowed to dry in a desiccator for 24 h before examining at the acceleration voltage of 80 kV (Hitachi, HT7700, Japan).

3.3.6 Drainage Test

To evaluate the draining ability of the slurries or suspensions of BG, BG/NFC, BG/mNFC and BG/NFC+CPAM, each sample was diluted to 0.2wt% solid content and mixed by a homogenizer for 5 min (according to TAPPI T221). Then, water was drained off the suspension under a vacuum through a 0.45 μm Durapore PVDF membrane filter. A standard stop-watch was used to record the draining time (sec) which was assumed to be completed when the time difference between the consecutive drops falling from the glass funnel connected with a vacuum was more than 30 sec.

3.3.7 Scanning Electron Microscopy (SEM)

The surface morphology of molded sheet samples was observed at an accelerating voltage of 10 kV by using SEM (LEO/1450 VP, USA). All samples were cut into 5 mm x 5 mm and coated with gold before observed.

3.3.8 Grammage and Density Measurement

The grammage of prepared sheets were measured in unit of gram per square meter (g/m^2). Each molded sheet was prepared into a size of 150 mm ×150 mm before pre-conditioned at room temperature (RT), 50% relative humidity (RH), for overnight before weighing (TAPPI T410). A 5 random positions of samples were measured for thickness using a digital Vernier caliper. Then, the average density values of the sample sheets were calculated by its weight and dimension (mass/volume).

3.3.9 Tensile Testing

Testing was performed according to TAPPI T494 by using a universal testing machine (Instron Model 5566, USA, 1 kN load cell equipped). The sheet samples with a size of 1.5 cm × 8 cm and gauge length of 5 cm were pre-conditioned at 50% RH and 25 ºC overnight before the test. The testing speed of 7 mm/min was applied and at least 7 specimens were tested for each sample. The average tensile strength (UTS), modulus of elasticity (MOE), and elongation at break (EAB) of the sheet samples were evaluated subsequently from the test results.

3.3.10 Water Contact Angle

The surface wettability of each sheet sample was estimated by contact angle measurement (KINO, SL200KS, USA). The sheets were cut into small pieces of about 10 mm x10 mm. A droplet of water (5 μl) was then deposited on the specimen surfaces and the contace angle was measured at 0.1 sec after drop deposition. To reduce a possible influence of the surface heterogeneity, a minimum of ten readings were taken on each sample.

3.3.11 Oil Resistance

The oil wettability of all samples was studied using the dynamic contact angle (SL200KS, KINO), in which oil was observed on the sample surface. Before testing, the sample sheet was prepared to 10-20 mm^2 and condition in a desiccator for 24 h. A 10 μl of oil was dropped on the sample surface. The drop measure within the first 0 seconds, and each measured at least 10 times to reduce the error from the sample inhomogeneous. Moreover, dynamic oil contact angle change was measured by recording the contact angle change of an oil drop with time within 11 seconds at room temperature with 50% RH. Oil penetration behavior of uncoated and coated BG molded pulp samples was investigated obviously from the photograph. Both of sample was observed with 100 ml cooking oil (palmitic oil) at room temperature. The testing started from oil was poured into the molded pulp sample, took a photo for the penetration characteristic at starting time, and then started the stopwatch immediately. After 30 minutes, the oil was removed from the molded sample, and observed the different

characteristics of oil penetration within the sample of uncoated and coated molded pulp packaging [128]. The grease resistance was determined by the Kit test (standard TAPPI T 559 cm-12) which was widely used in oil-proof paper and paperboard industry at present. In this method, 12 kinds of liquid were prepared using castor oil, toluene, and n-heptane (Table 3.2). The test solution was prepared in accordance with the above-mentioned standard. Results were recorded as kit number from 1 to 12.

Table 3.2 Kit Test Standard Solutions

Reagents	**Kit number**											
	1	**2**	**3**	**4**	**5**	**6**	**7**	**8**	**9**	**10**	**11**	**12**
Castor oil (ml)	200	180	160	140	120	100	80	60	40	20	0	0
Toluene (ml)	0	10	20	30	40	50	60	70	80	90	100	90
Heptane (ml)	0	10	20	30	40	50	60	70	80	90	100	110

3.3.12 Thermogravimetric (TGA) Analysis

The thermal stability of the uncoated and coated samples was determined by the thermogravimetric analyzer (Model 851e, Mettler Toledo, USA). The samples were cut into a small piece and placed in an aluminum. The mass of the samples was generally in the range of 5-10 mg. The sample was run under an N_2 atmosphere by using a flow rate of 10 ml/min, temperature heated from room temperature to 700 °C.

3.3.13 Water Vapor Transmittance Rate (WVTR)

The WVTR of all sheet samples were evaluated according to ASTM E96/E96M procedure. Each sample sheet was cut into circles of approximately 8 cm diameter and mounted onto a circular aluminum cup. Beforehand, 10 g of desiccant silica gel was added to the cup. Beeswax was used to fixate the sheet sample tightly against the cup. After that, each sample cup was weighed for the first time with an analytical balance and then placed in a vacuum desiccator chamber under testing conditions of 25°C and

70% RH with a continuous air circulation. Weighting was repeated until constant weight to determine the amount of vapor transferred into the desiccant. WVTR was later calculated from the following equation:

$$WVTR = \frac{Wv}{t \times A}$$

where Wv is the amount of water vapor (g), t is the time (days), and A is the sheet area (m^2).

3.3.14 Oxygen Transmittance Rate (OTR)

The oxygen barrier testing was referred from the method in ASTM standard D3985-02 (Model 8001, llinois, USA) which the value was reported to oxygen transmission rates (OTR). Tests were carried out at 23°C and 0% RH with 99% oxygen as a test gas. A coulometric sensor measures the oxygen that is transmitted through the material. Aluminum foil masks, with an inner diameter of 5 cm^2, were used to mount test pieces in the diffusion cell. The readings were corrected to 1 atm partial pressure gradient of permeant gas.

3.3.15 Statistical Analysis

To differentiate the data or results from the water absorption and tensile testing, a randomized complete block design (RCBD) method was used to statistically analyzed the data with the STAR program. The average values were reported from a significant level less than 0.05 ($p<0.01$).

CHAPTER 4

RESULTS AND DISCUSSION

4.1 Molded Pulp Integrated with Modified Nanofibrillated Cellulose (mNFC)

4.1.1 Modification of NFC at Different Sonication Amplitude and Time

In this work, NFC was modified via esterification reaction using lactic acid. The change in chemical structure after modification was confirmed by FTIR spectra in Figure 4.1. The unmodified NFC showed the characteristic bands corresponding to the stretching mode of C-H of hydrocarbon at 2086 cm^{-1} [129]. For both NFC and mNFC samples, a broad characteristic absorption peak of O-H at 3336 cm^{-1} can be found, attributing to the stretching induced by hydrogen bonds, while a small peak at 2901 cm^{-1} was observed, corresponding to the stretching vibration of methyl and methylene C-H bonds in cellulose. The characteristic bands at 1642 and 899 cm^{-1} denoted the vibration of H-O-H absorbed water molecules and β-glycosidic linkages between glucose units, respectively. Upon NFC esterification, a strong stretching vibration peak at 1745 cm^{-1} (assigned to ester C=O moieties) appeared in all mNFC samples, confirming the successful modification of NFC after esterification process. With the increase of sonication amplitude during reaction (percentage from mNFC30 to mNFC90), the relative intensity of the ester peak gradually increased. Also, the intensity of the band corresponding to asymmetric bending of CH_3 appeared at 1370 cm^{-1} and the bands appeared at 1229, 1118 and 1031 cm^{-1} representing symmetric and asymmetric of C-O-C stretching modes were found to increase [130]. Furthermore, a reduction of the intensity of the band associated with the vibration of OH groups (at 3336 cm^{-1}) implied the substitution or replacement of a fraction of hydroxy groups that took place in the mNFC samples.

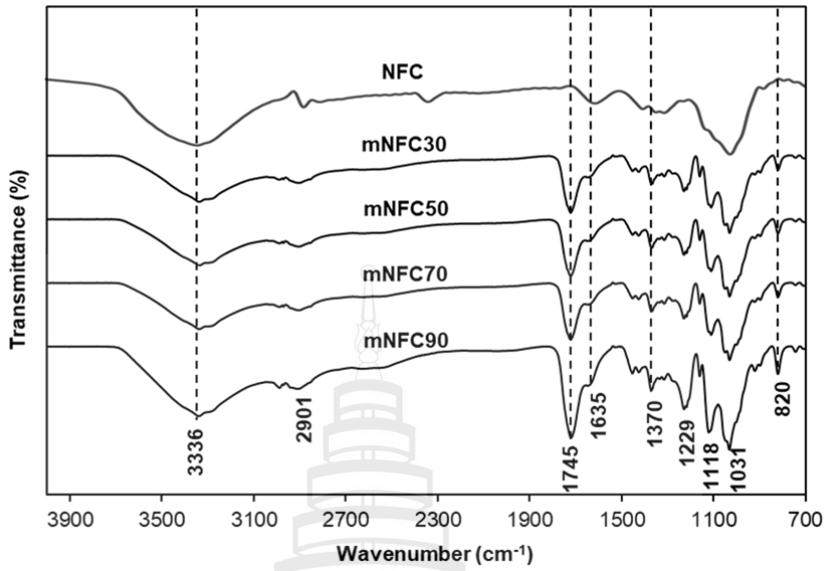

Figure 4.1 The Spectrum of Unmodified NFC (Reference) and Modified NFC (mNFC) Prepared at Different Sonication Amplitudes of 30-90% during Esterification Reaction by FTIR Testing

The degree of substitution (DS) of all mNFCs are presented in Figure 4.2, with sonication energy calculated based on various sonication amplitudes and times employed during the reactions. With 10 min sonication time, the DS of mNFCs increased linearly with increasing sonication amplitude percentage from 0.21, 0.34, 0.41 to 0.55 for mNFC30, mNFC50, mNFC70, and mNFC90, respectively. This implies that the increase in reaction amplitude or energy has led to an increase in cavitation during reaction, leading to activated reagents and enhanced chemical reactivity [131-134]. In addition, with increased sonication energy, NFC might become finer hence having a higher specific surface area with increased amount of OH groups accessible for esterification reaction. When the amplitude is fixed at 90% and the sonication time was increased to 30 and 60 min, the calculated energy for the reaction increased tremendously, however, the DS was found to be slightly decreased. This is believed due to the lengthen reaction or excessive sonication which might cause a reverse in the esterification reaction of NFC [131] while the NFC might get damaged during the course of the reaction.

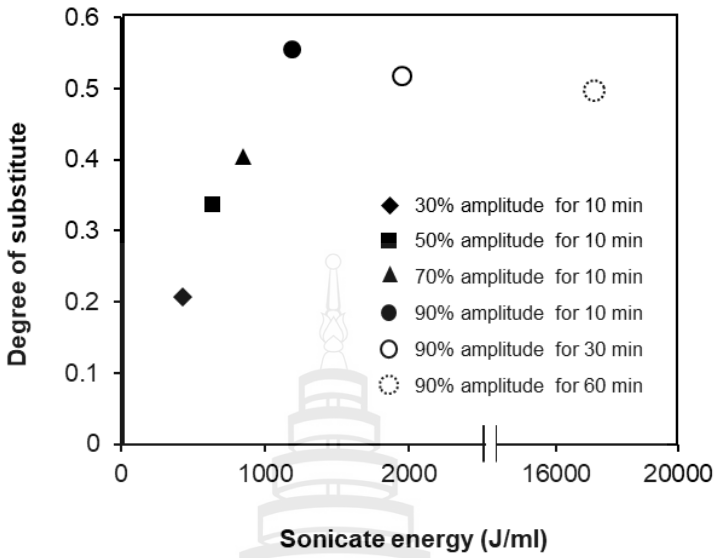

Figure 4.2 Degree of Substitution (DS) of the mNFCs Prepared at Different Sonication Amplitudes and Times Determined by a Back-Titration Method

The proposed mechanism of the NFC modification reaction is shown in Figure 4.3. With the applied energy from sonication, initially, hydroxy radicals are generated from water molecules which can then further react non-selectively. The hydroxy radicals can capture hydrogen atoms on both lactic acid and NFC, leading to generation of radicals on lactic acid and NFC structures. When both radicals react, the esterification occurs and then propagates which possibly creates oligomer of lactic acids on the surface of NFC as later suggested by C^{13} NMR (Figure 4.4) [135-136]. Three hydroxy groups in the cellulose structure including the primary hydroxy group at C6 and secondary hydroxy groups at C2 and C3 can all possibly participate in the esterification reaction [132]. However, the hydroxy group at C6 in the repeating unit of cellulose is expected to be the most reactive site for the reaction, since only C6 hydroxy are oriented outwards from the surface of the nanofibers [137]. Between secondary hydroxy groups of C2 and C3, the secondary hydroxy group of C2 might also have a higher possibility to participate in the reaction than that of C3 as a result of the intramolecular hydrogen bonds formed at the position of C3 hydroxy groups [138].

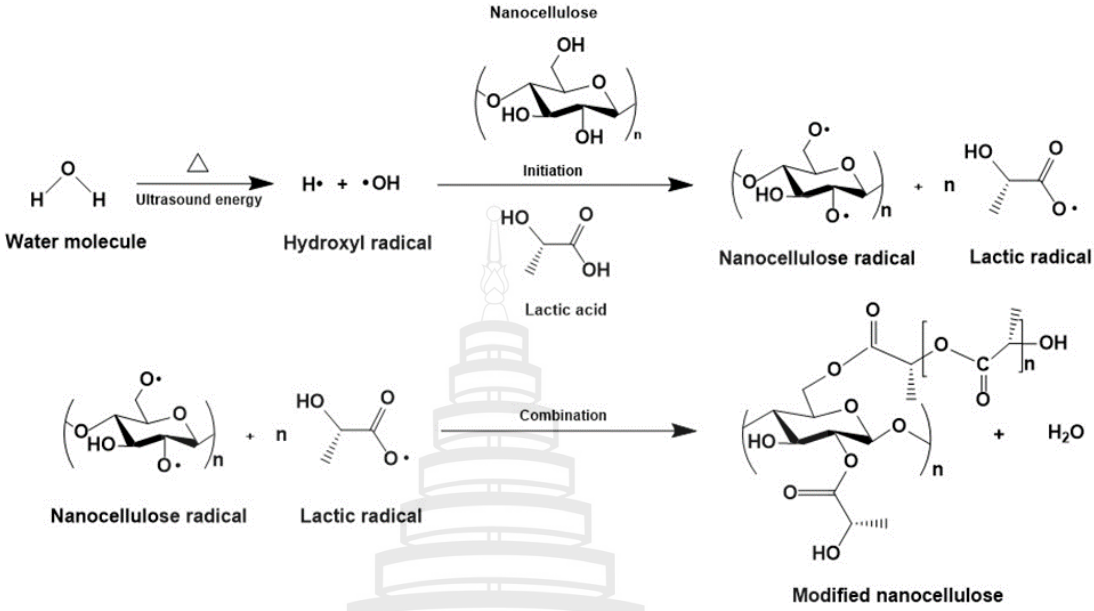

Figure 4.3 Proposed Mechanism for The Esterification of NFC with Lactic Acid in Water Medium, Accelerated by Sonication Energy

The solid-state ^{13}C-NMR spectra of unmodified NFC and mNFCs prepared at different sonication amplitudes (mNFC30, mNFC50, mNFC70, and mNFC90) are shown in Figure 4.4A – 4.4C. All samples showed the signals at δ_C 106.5, 70.1, 72.5, 88.5 and 66.5 ppm which were assigned to the carbon peaks on the glucose rings at C1, C2, C3, C4, C5 and C6, respectively [139]. In the mNFC30 (DS 0.21) and mNFC50 (DS 0.34) spectra (Figure 4B), the new peaks of three carbonyl carbons (C=O) at δ_C 169.4, 173.6 and 175.5 ppm can be found, while the overlapping chiral methine carbons (CH) of lactide with those of NFC were shown at δ_C 69.7 ppm and the methyl groups (CH_3) appeared highfield at δ_C 16.7 and 20.0 ppm [134]. These results further confirmed the successful esterification process of the mNFC. Since the methyl group of lactic acid should only appear as a singlet at around δ_C 16.7 ppm, these two methyl signals at δ_C 16.7 and 20.0 ppm suggested the presence of oligomer of lactic acids in these mNFC samples. On the other hand, for the mNFC70 (DS 0.41) and mNFC90 (DS 0.55) samples (Figure 4.4C), the carbonyl carbons were observed with four positions at

δ_C 169.4, 173.6, 175.5 and 178.2 ppm. The stronger overlapping peaks of chiral methine carbons and methyl groups however appeared at the same positions as did in the spectra of mNFC30 and mNFC50. This result indicated that not only DS of mNFCs was increased with increasing sonication amplitude during the reaction but also the length of lactic acid oligomers substituted on the current mNFCs [140-141].

The XRD patterns obtained from NFC and mNFCs are shown in Figure 4.5. All samples exhibited the typical diffraction of native cellulose I at the main angle (2θ) at around 22º (002)). When the sonication amplitude percentage used in reaction to prepare mNFCs increased, a clear decreasing and broadening trend of all peak intensities was observed. From the titration results, it was found that when the higher sonication amplitude was used, the mNFCs with higher DS were obtained ranging from DS of 0.21 (mNFC30) to DS of 0.55 (mNFC90). This clearly indicated that the more substituted units on mNFC chains, the more cellulose crystalline structure was disrupted and then converted to amorphous phase. In addition, it was possible that the hydrodynamic forces associated with ultrasound during sonication could do damage to the crystalline domains of mNFC samples [142-143]. The crystallinity index (CI) calculated from their diffractograms was also shown to be decreased gradually with increasing sonication energy. A similar decline in CI of cellulose nanocrystals (CNCs) dispersed in aqueous PVA matrix as ultrasonication treatment time and amplitude increased was reported by Shojaeiarani et al. 2020 [120].

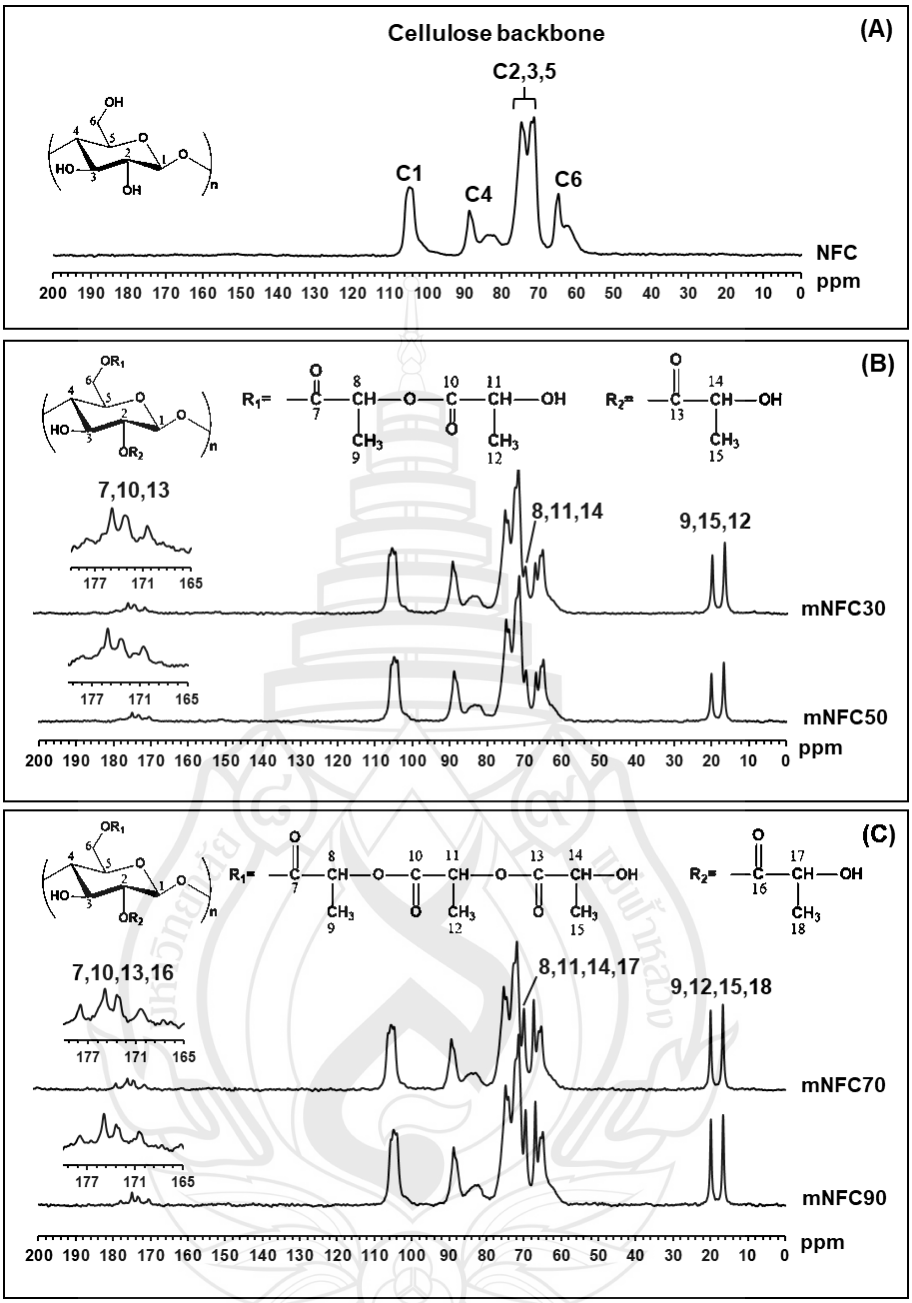

Note The structural formula shows the characteristic carbons of the anhydroglucose unit in cellulose (nfc) and the appearance of characteristic carbon of c=o, ch and ch_3 indicating the lactic acid substitution in mnfc samples

Figure 4.4 Solid-state ^{13}C-NMR Spectra of (A) NFC; mNFCs Prepared at (B) 30% and 50% Amplitude and (C) 70% and 90% Amplitude

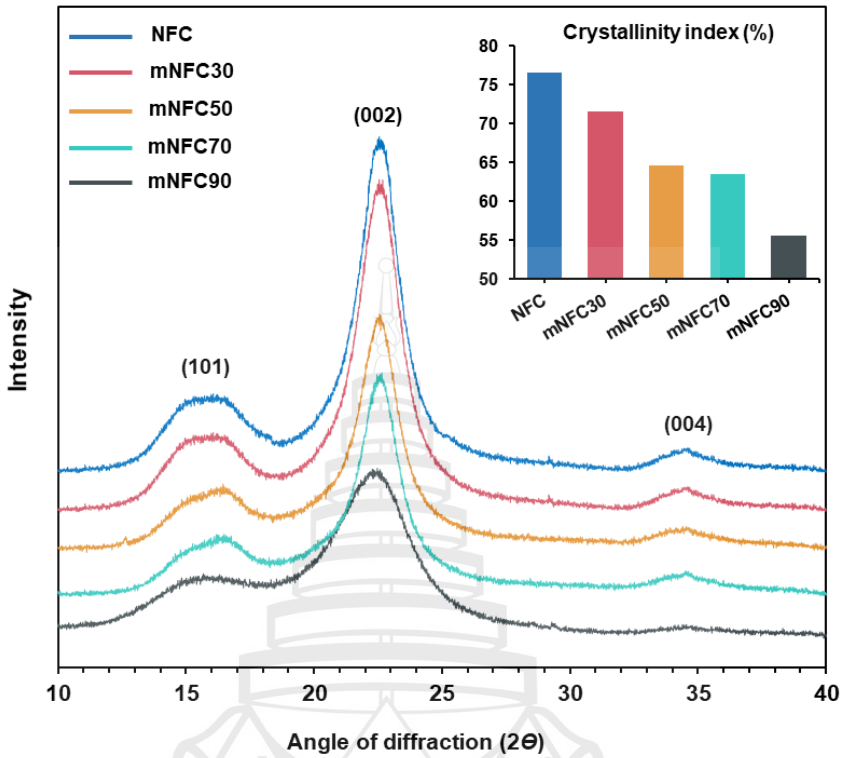

Figure 4.5 X-Ray Diffraction Patterns and Crystallinity Indices (Inset) of NFC and mNFCs Prepared at 30-90% Sonication Amplitudes

From TEM images in Fig 6, the unmodified NFC (Figure 4.6A) showed a typical characteristic of long fibrillated cellulose nanofibers. After the sonication-assisted modification reaction, the morphology of the mNFC nanofibers appeared to change progressively. For the mNFC30 sample, the fibrillated portions around the main nanofibers were largely removed and became more like individual nanofibers with clean surfaces (Figure 4.6B). At higher sonication energy condition (mNFC90), rod-like small fragments were observed together with the main cellulose nanofibers (Figure 4.6C). This suggested that the sonication power not only disrupted crystalline region in mNFCs but also induced the shearing stress which led to a partially hydrolysis of cellulose and size-reduced the nanofibers into smaller fragments [144]. As a result, the initial crystal structure of NFC was therefore diminished to certain extent, in agreement with the XRD results as presented earlier.

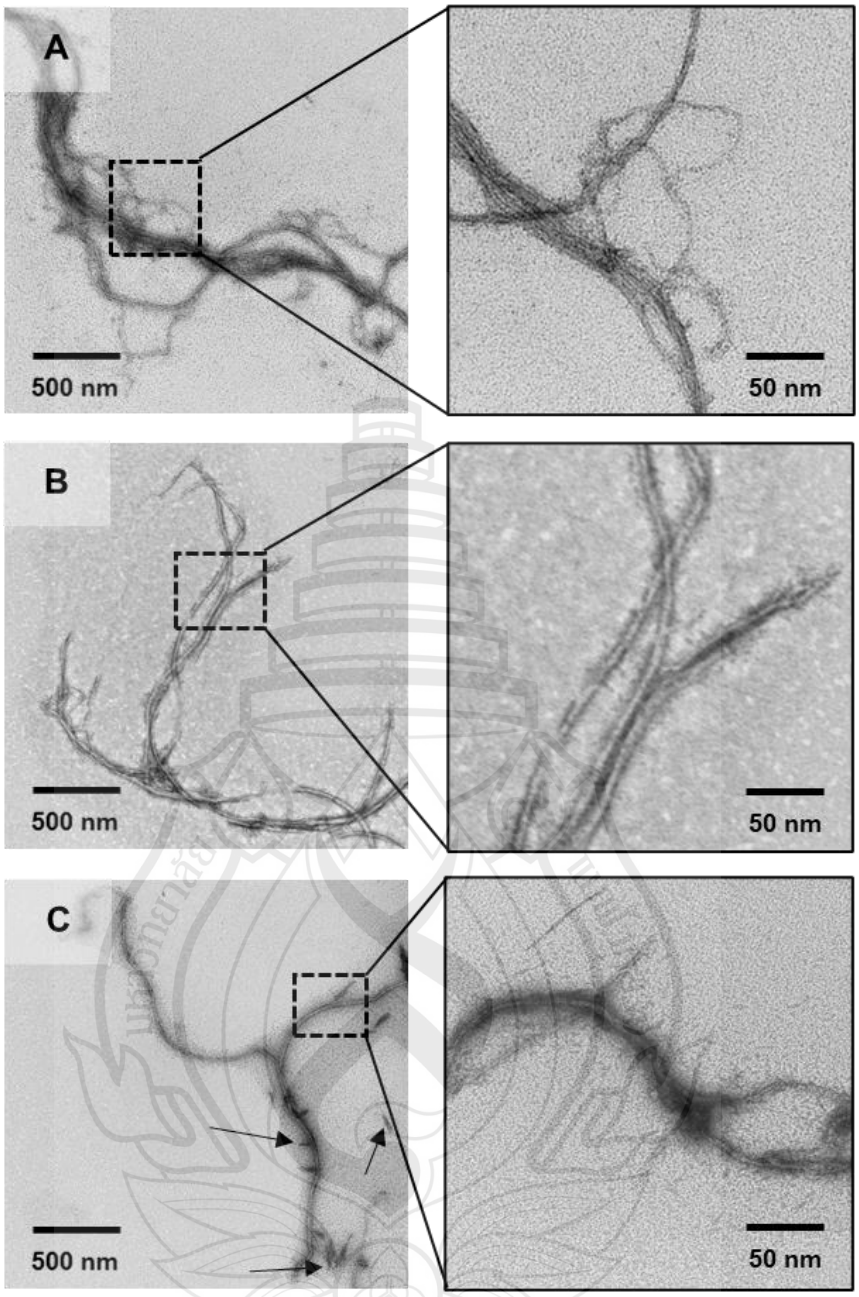

Figure 4.6 TEM Images of **(A)** NFC, **(B)** mNFC30%, and **(C)** mNFC90%, the Fragmented Parts from the Main Nanofibers Indicated by Black Arrows. Partial Enlargements of (A), (B), and (C) are in the Right Column

4.1.2 Integration of NFC, mNFC in Molded Pulp Sheets

To form a molded pulp, the draining of water from the pulp slurry using vacuum assisted system is required before hot-pressing the dewatered pulp into a desired shape. In this study, when NFC (5 wt%) was added into the BG pulp slurry, a substantial delay in drainage was recorded (Figure 4.7A). This is due to an extremely high specific surface area of NFC containing numerous hydroxy groups, resulting in extremely high-level hydrophilicity with extensive interactions with water molecules [145-146]. Moreover, anionic charges on both NFC and BG cellulose pulp creates an electrostatic repulsion that pushes away NFC from the network of BG pulp fibers [147-148]. As a result, a major portion of NFC integrated with the draining flow and started to block porours structures of the water flow channels, delaying the drainage process (Figure 4.7B). In the real production or manufacturing molded pulp packaging which normally is in a many million pieces per day scale, if the forming and dewatering time (one of the main step processing times) increases to double, the production rate could be seriously declined [149]. Furthermore, during the vacuum drainage process, certain amounts of NFCs could be forced to penetrated through the filtering layer, hence leading to a partial loss of NFC contents in the final BG/NFC molded sheets.

With mNFCs addition, the draining time was evidently reduced as compared to the NFC system. This is believed due to the lactic acid oligomers on mNFC surfaces which can provide a bulky effect to expand the flow channels for drainage (as illustrated in Figure 4.7B). These substituted oligomers are more hydrophobic than hydroxy groups, leading to a reduced water bonding capability [150]. As expected, the mNFC90 with more substituted ester groups (DS 0.55) and longer oligomer chains showed a greater effect on drainage than the mNFC30 (DS 0.21), with a much-shortened drainage time of 10 seconds only. On the other hand, the addition of CPAM also showed a positive outcome on drainability of the BG/NFC system. This was attributed to the positive charge of CPAM that can bind NFC to the BG pulp fibers and thus enable the retention of NFC in their microfiber network, providing the flow pathways for water to drain off [151]. After the statistical analysis, it was found that the positive influence of CPAM addition on the draining time of the BG/NFC system was

less but not significantly different ($p < 0.01$) than using the modified nanocellulose or mNFC90 alone.

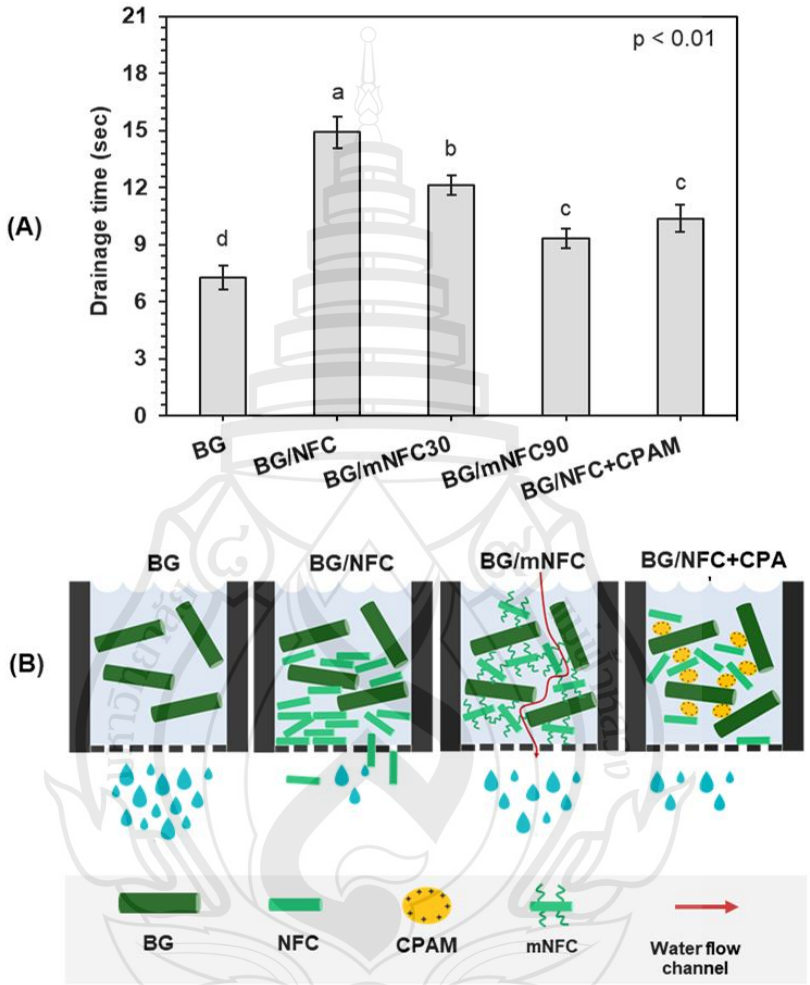

Figure 4.7 Comparison of Drainage Time in The Different Systems; BG Pulp Slurries with NFC, mNFCs, and NFC+CPAM. The Values Represent Means ± SD of Four Replicates. Means with Different Letters Indicate the Statistically Different Data Groups Based on ANOVA Test ($p < 0.01$) (A). Illustration Explains the Effect of NFC, mNFC, and CPAM Addition on Dewatering of the Slurries During Vacuum (B)

After forming molded pulps, the surfaces of the prepared sheet samples were observed. As shown in Figure 4.8, the pure BG sheet surface (Figure 4.8A) showed typical micro-sized cellulose fiber morphologies with certain overlapping as well as some gaps between microfibers and bundles. With the addition of NFC (5wt%), traces of finer networks of possible fibrillated nanofibers were obtained on the surface of the BG/NFC sheet (Figure 4.8B). On the other hand, the surfaces of the BG sheets integrated with either mNFC90 or NFC+CPAM were found to be much smoother and denser with less porous features when compared to the previous sheets. It seemed that, for these two sheets (Figure 4.8C and 4.8D), mNFC and NFC could be retained more on their surfaces so the nanofiber networks bridged the microfibers, therefore, filling and closing those gaps [152-153].

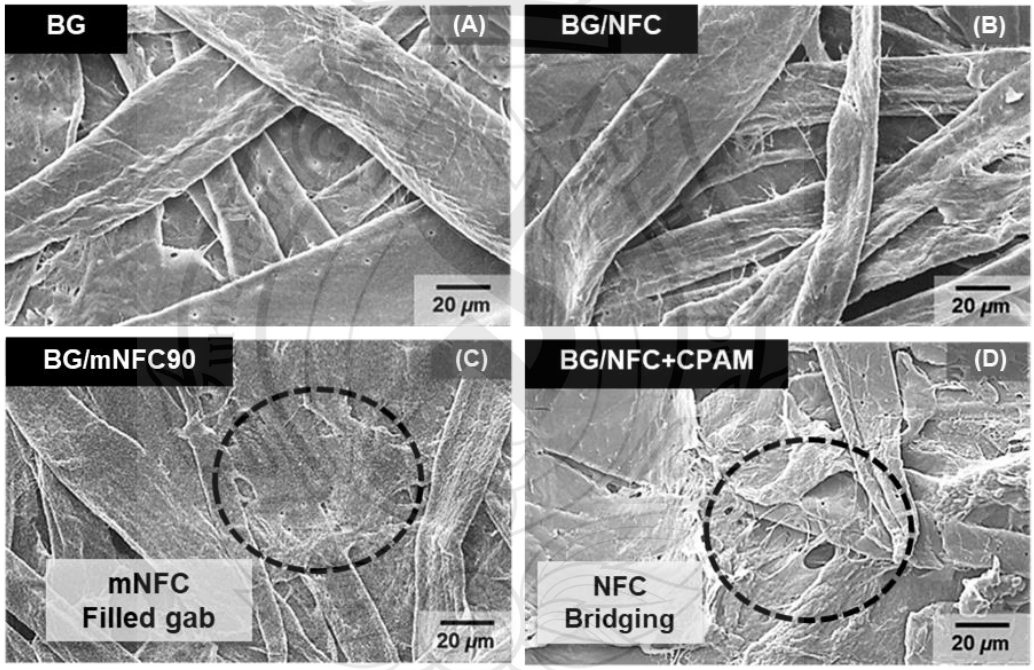

Figure 4.8 SEM Photographs of the Surfaces of (A) Pure BG Sheet, (B) BG/NFC, (C) BG/mNFC90%, and (D) BG/NFC+CPAM. The Circles Indicate the Retaining NFC and mNFC that Bridges Between the BG Microfibers and Fills Up Gaps on the Sheet Surfaces

From Table 4.1, both the areal weight and density of the BG-based sheets shown a slight increase with addition of 5 wt% of NFC. At the same content of mNFC, the grammage and density slightly increased with higher amplitude of sonication process, further indicating an increase in the final solid content and confirming the retention of added nanofibers in these sheets [154]. With these increased sheet densities, an expected improvement in tensile strength (UTS) of around 10 MPa based on a typical strength of cellulose nanopaper (~200 MPa) and composite rule of mixture (ROM) was obtained only in BG/mNFC sheets [155-156]. This is attributed to the retained nanofibers which can promote the contact areas between BG microfibers and increase the number of hydrogen bonding (inter-fiber bond density) and inter-fiber bond strength within the structures, facilitating stress tranfer in cellulose networks and providing reinforcement to the sheet properties [157-159]. Although the mNFCs were modified or partially substituted with ester groups which can lead to a slightly reduced hydroxy groups, the tensile properties of the BG/mNFC sheets were significantly higher than those of the BG/NFC sheet, confirming the remaining content of nanocellulose in the sheets should be predominant. The obtained improvement levels of mechanical properties are in good agreement with literature reporting paperboards with the addition of CNFs and modified CNFs (10 wt%). Nonetheless, the modulus of elasticity (MOE) of current mNFC integrated BG sheets were not reached an expectation (~1 GPa increment) considering the 5 wt% mNFC addition and possible contribution from a typical cellulose nanopaper's modulus (~20 GPa). The plausible explanation should involve the larger degree of deformation (strain) allowed from segment motion of molecules in amorphous region of nanocellulose fibers in these mNFC integrated samples. However, the deformation degree of cellulose nanopapers is still restricted since slippage and large-scale reorientation of cellulose nanofibers in the network were not likely to occur in a dry state [156].

When CPAM is added into the system with NFC, the density of the BG/NFC+CPAM sheet was increased slightly (Table 4.1). Its tensile strength and modulus were also found to increase in comparison to the BG/NFC sheet. Among all samples in this study, the highest elongation at break of the sheet with CPAM addition was observed. This enhancement is believed to originate mainly from a characteristic

of the CPAM polymer structure which increases free volume and, hence, degree of flexibility of the sheet [160]. In addition, the bridging between NFC-CPAM-BG microfibers might not be as strong as the secondary bonding between NFC-BG or mNFC-BG networks, therefore, allowing more deformation before breaking and a good measure of the sheet toughness [124].

Table 4.1 Grammage (GSM), Density (ρ), and Ultimate Tensile Strength (UTS), Modulus of Elasticity (MOE), and Elongation at Break (EAB) of the Sample Sheets

Sample code	G (g/m^2)	ρ (g/cm^3)	UTS (MPa)	MOE (GPa)	EAB (%)
BG	352	0.74 ± 0.02^{c}	28.36 ± 2.82^{d}	3.07 ± 2.75^{d}	1.67 ± 0.15^{e}
BG/NFC	354	0.78 ± 0.03^{b}	31.70 ± 2.65^{c}	3.15 ± 1.44^{c}	1.86 ± 0.19^{d}
BG/mNFC30	357	0.81 ± 0.04^{ab}	37.32 ± 1.98^{ab}	3.28 ± 1.79^{ab}	2.23 ± 0.27^{c}
BG/mNFC90	359	0.84 ± 0.03^{a}	39.12 ± 1.13^{a}	3.31 ± 2.98^{a}	2.60 ± 0.35^{b}
BG/NFC+CPAM	358	0.80 ± 0.02^{b}	35.59 ± 2.60^{b}	3.26 ± 2.61^{b}	3.43 ± 0.18^{a}

Water resistance of pulp products or surfaces is usually low due to the high affinity of cellulose structure towards water molecules. So, when adding NFC into the BG pulp sheet, the water resistance of the BG/NFC sheet surface or water contact angle was reduced (Figure 4.9A). This is due to the hydrophilic nature of NFC together with its exceedingly high surface area [161]. The addition of CPAM into the BG/NFC sheet increased the contact angle from 26º to 39º. One reason is because CPAM or cationic polyacrylamide is more hydrophobic than NFC [162]. Moreover, this polymer additive resulted in a denser sheet surface as seen in the SEM images (Figure 4.8).

For the BG specimens with integration of mNFCs, the existence of hydrophobic substituted groups of ester oligomer chains on the nanocelluloses led to a clear effect on the surface water resistance of the BG/mNFC sheets. A contact angle of 52º was obtained, showing an over 70% increase compared with pure BG specimens. As

expected, higher contact angles were obtained from mNFC90 with higher DS than the mNFC30. The water vapor transmittance rate (WVTR) results are presented in Figure 4.9B, showing a good agreement with the water contact angle data. After statistical analysis, it was found that only the BG/mNFC90 sheet had a significant improvement in water vapor barrier properties ($p<0.01$) when compared to the other sheets. Thus, it should be noted that the degree of modification or ester group substitution on NFC is rather important when water barrier properties of the sheets are relevant to applications.

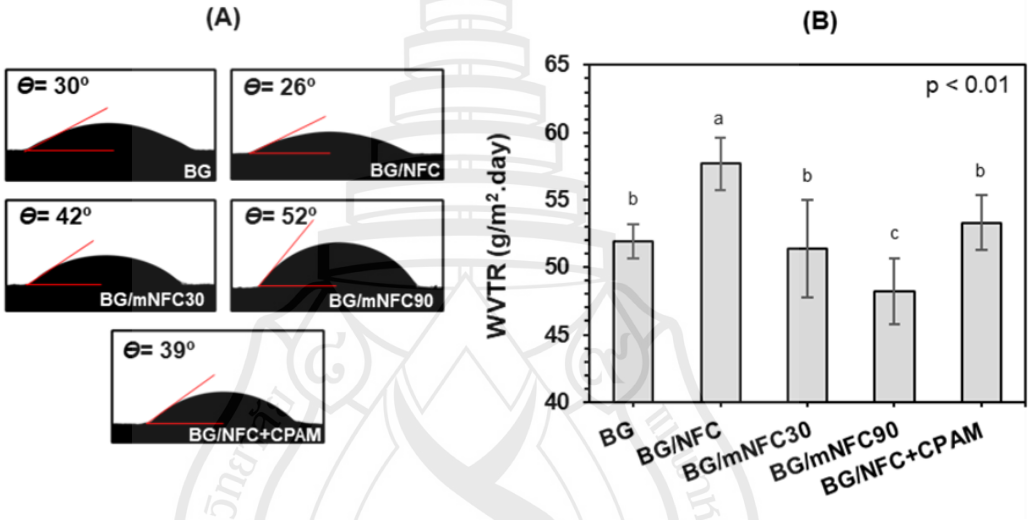

Figure 4.9 (A) Water Contact Angle on Surfaces and (B) Water Vapor Transmittance Rate (WVTR) at 70% RH of the Pure BG Sheet Compared to Other Sheets Integrated with NFC, mNFCs, and NFC+CPAM

4.2 Molded Pulp Coated Nanocomposite Film of Modified Nanofibrillated Cellulose (mNFC) and Shellac

4.2.1 Viscosity, Thickness and Cross-Section Morphology

From Figure 4.10A, the pure shellac solution (S) showed viscosity equal to 10.1 mPa.S and increased when increasing nanocellulose. The film thickness increased linearly with the viscosity, as shown in Figure 4.10B. The coating film thickness was calculated to an estimation of 100 μm based on shellac; however, the thickness of S

coating layer was measured to be around 40-50 μm. It should be because the shellac solution has low viscosity hence easy to flow and penetrate through pores between BG microfibers [163]. It can be observed that the cross-sectional SEM images of shellac coated BG sheet (BG/S) had less pores (Figure 4.10D) compared to uncoated BG sheets (Figure 4.10C). Indeed, the shellac solution filled pores between BG fibers [164-165]. The viscosity of S-NFC1 and S-NFC5 solutions was equal to 25.3 mPa.S and 30.2 mPa.S, respectively. The thickness of both conditions increased to 71 μm and 111 μm. This should be because the nanocomposite solution has a higher resistance to flow into BG sheet making the solution less penetrable and thicken on the sheet surface (Figure 4.10E) [166-168]. BG/S-mNFC1 and BG/S-mNFC5 solution showed the viscosity of 27.6 mPa.S and 32.4 mPa.S, respectively. The solution with mNFC addition presented higher viscosity than those with NFC addition possibly because the mNFC had oligomer units on their surface [169]. The similar results were explained by Yook et al. that the modified NFC had low hydrogen bonding between mNFC-mNFC fibers because the ester functional groups showed electrostatic repulsion [170]. Consequently, the mNFC obviously increased coating thickness (Figure 4.10F) on the BG surface than the NFC coating system.

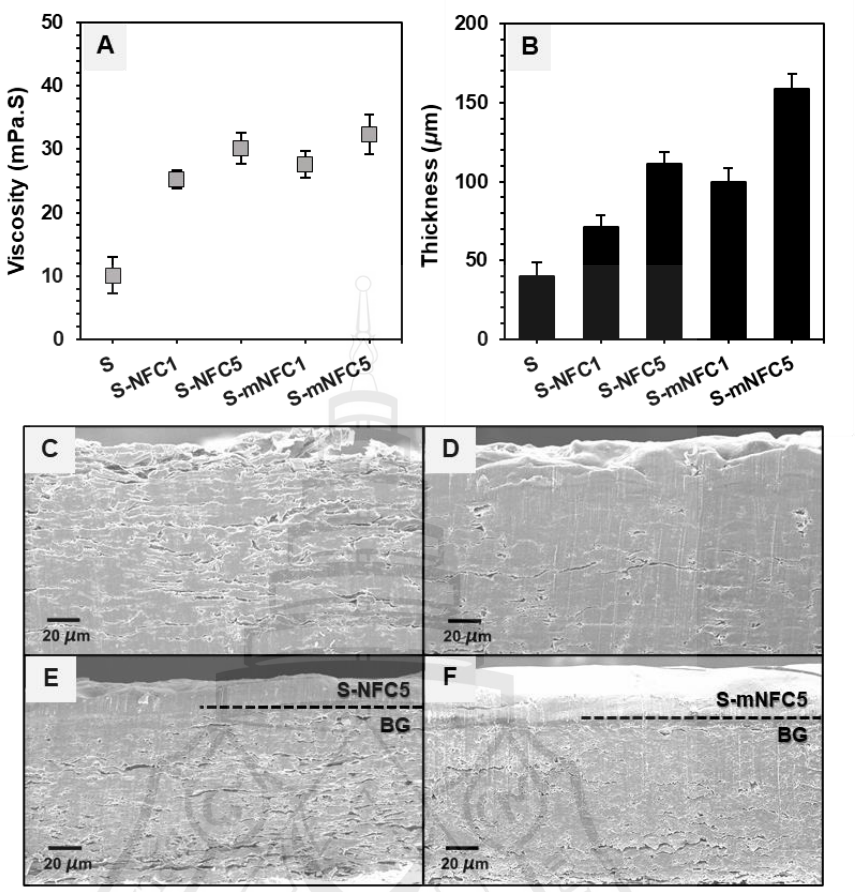

Figure 4.10 (A) Viscosity of Nanocellulose/Shellac Coating Solution, (B) Thickness of Coating Layer and (C)-(F) Cross Sectional Morphology of Uncoated BG Sheet and Coated BG Sheet with Different Coating Conditions; (C=BG; D=BG/S; E=BG/S-NFC5; F=BG/S-mNFC5

4.2.2 Oxygen Barrier

Figure 4.11 showed the oxygen transmission rate (OTR) of the uncoated BG, shellac coated and nanocomposite coated BG samples. The uncoated BG sheet showed the highest OTR of 2,338 cc/m^2-day. The micro-sized fibres in pulp and paper materials made them had many gaps between fibres on surface observed by SEM image (see Figure 4.12A) and oxygen can easily pass through [171]. When, shellac coated on BG the OTR was decreased slightly. From SEM images, it was observed that shellac could cover all surface of the BG sheet, showing a smooth surface (see Figure 4.12B).

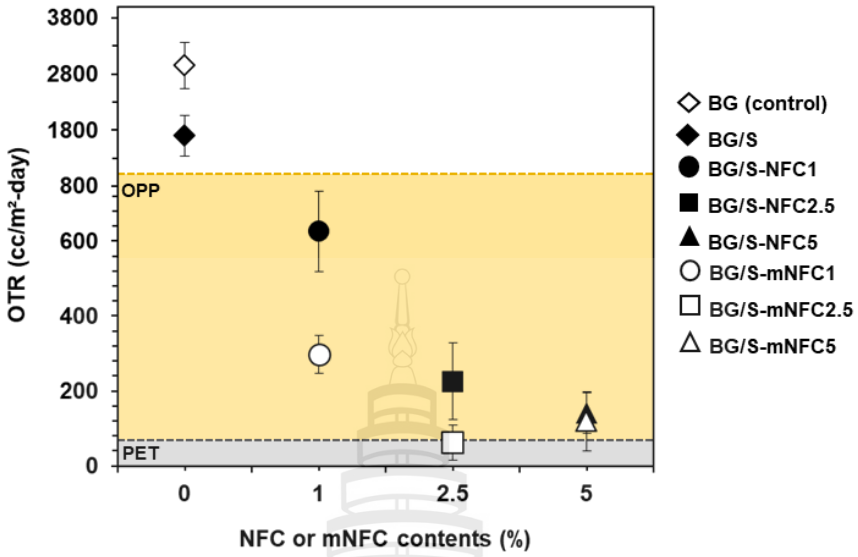

Figure 4.11 Oxygen Transmission Rate (OTR) of Uncoated BG Sheet and Coated BG Sheet with Different Coating Conditions (OPP; Oriented Polypropylene and PET; Polyethylene Terephthalate)

For the NFC nanocomposite coated samples, all conditions (BG/S-NFC1, BG/S-NFC2.5, and BG/S-NFC5) showed the decreasing OTR results compared to BG and BG/S. The function of NFC in the composite is to promote a long pathway that could slow gas transfer inside [172-173]. However, when NFC content increased from 2.5 to 5 wt%, the OTR result presented did not change much. Perhaps, it was due to an partially agglomeration of NFC by a strong hydrogen bonding among them. Figure 4.12C and Figure 4.12D showed that the BG/S-NFC5 had many white spots on surface indicates higher possible agglomeration occurred than in BG/S-NFC1 [174]. On the other hand, a coating layer of mNFC nanocomposite on BG sheet displayed the greater degree of decreasing OTR value. The condition of 1% and 2.5% mNFC contents showed an OTR of 379 cc/m^2-day and 61 cc/m^2-day, respectively. This effect should be contributed to a good mNFC dispersion in the shellac because of less self-agglomeration [175-176]. However, the 5% mNFC showed a slightly increased OTR value. These results again suggested the possible occurrence of mNFC agglomeration at high contents and the optimum value was 2.5% mNFC loading content for this

system. As compared the BG/S-mNFC2.5 showed the OTR value better than OPP and close to PET plastics to commercial packaging.

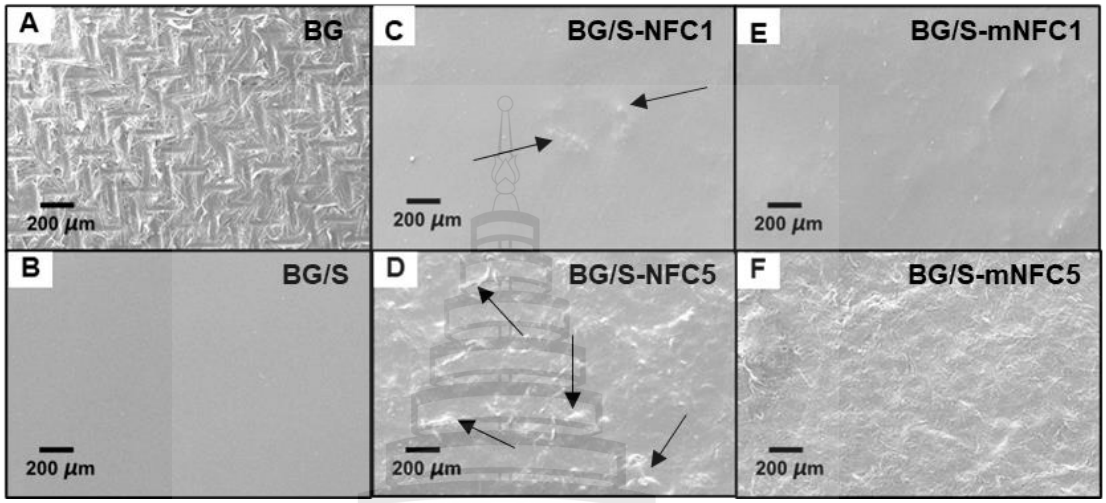

Figure 4.12 The SEM Surface Morphology of (A) BG Sheet, (B) BG/S, (C) BG/S-NFC1, (D) BG/S-NFC5; Black Arrow Indicated the NFC Agglomeration, (E) BG/S-mNFC1; (F) BG/S-mNFC5

4.2.3 Water Vapor Barrier and Water Resistance

From Figure 4.13A, the condition of the uncoated BG sheet shows the highest WVTR of 58 g/m^2-day. The WCA on BG was determined to be 34.5º. A surface is considered hydrophilic when the contact angle of water on its surface is <90º. When shellac coated on BG sheet (BG/S), the WVTR decreased by 80% and down to 17 g/m^2-day (compared to the uncoated BG sheet), and WCA increased to 67.2º. This result confirms the hydrophobic nature of the shellac (Figure 4.13B) [177]. However, BG/S-NFC1-5 presented the increasing value of WVTR and WCA compared to the BG/S condition. The NFC has an abundant hydroxyl group on the surface caused by the high surface area of nanofiber [178], hence, the hydrophilicity of NFC attracts and allows water molecules to pass through.

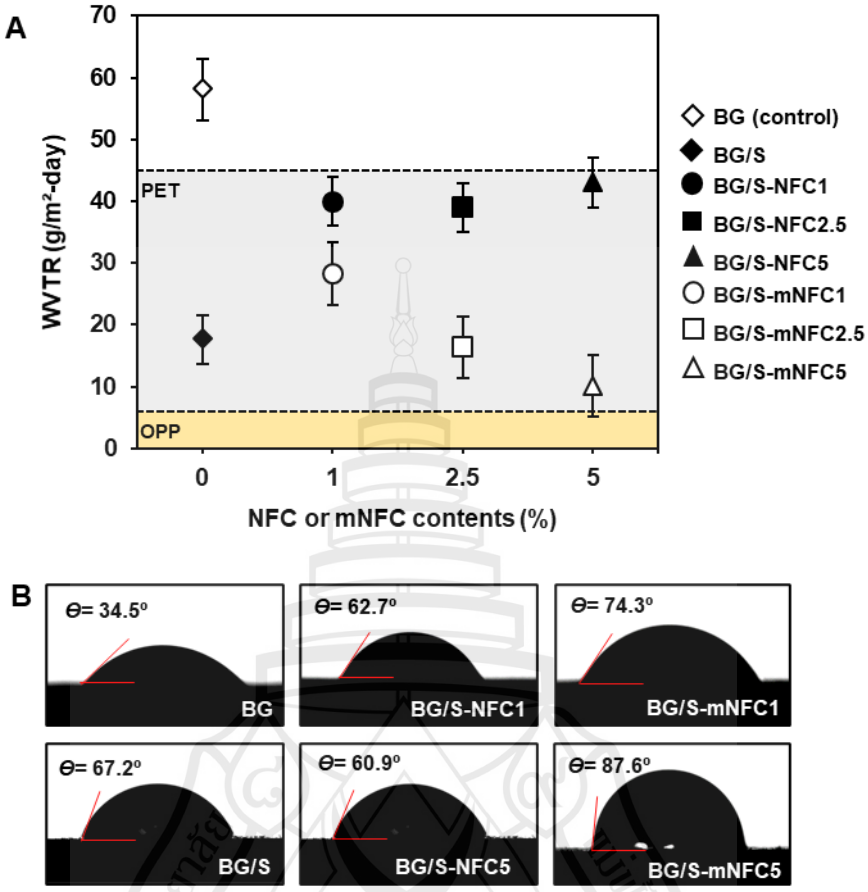

Figure 4.13 (A) Water Vapor Transmission Rate (WVTR) and (B) Water Contact Angle (WCA) of Uncoated BG Sheet and Coated BG Sheets with Different Coating Conditions

According to Lavoine et al., they found that hydrophilic NFC showed strong heterogeneities with hydrophobic shellac at the interface and made the film generate the nanopores [179]. The WVTR of BG/S-NFC2.5 and BG/S-NFC5 was not decreased, although the higher NFC dose was added to the shellac matrix. On the other hand, the mNFC content of 2.5% and 5% further decreased WVTR of the coated sample to 16.40 g/m^2-day and 8.64 g/m^2-day, respectively. These results demonstrated that the chemical modification of mNFC promoted a hydrophobic ester functional group which provided better dispersion and interface with shellac, and they prevented the transportation of water vapour [180]. BG/S-mNFC5 samples had a great increase in WCA to almost 90º.

Similar results with Yook et al., the coating surface of modified NFC (by silylation) presented strong hydrophobicity on the surface of base paper [181]. As compared to commercial packaging materials, the lowest WVTR value of BG/S-mNFC is close to that of OPP and PET packaging.

Table 4.2 showed different coating compositions and coating layer numbers of other research studies. The coating composition of single-layer micro- or nanocellulose was not enough to improve WVTR and OTR compared to bio-nanocomposite coating composition because of the combination of water resistant biopolymer and protective function nanofiller. In part of bilayer coating, it showed good WVTR from the main effects of water resistant biopolymer, but OTR was not good because of poor dispersion of nanolayer. Moreover, bio-nanocomposite layer in this thesis showed lower WVTR and OTR than other works due to the preformed coating technique and modification of nanocellulose.

Table 4.2 Comparison of Barrier Properties Based on Paper Material Depending on Coating Composition and Coating Process

Substrate	Coating composition	WVTR	OTR	Ref.
Single layer micro- or nanocellulose coating				
PB 178 g/m^2	MFC	4571	-	[182]
LB 180 g/m^2	NFC	200-300	>10000	[183]
LB 180 g/m^2	NFC carboxymethyl	280	7000	
WFP 215 g/m^2	NFC	250	>10000	[184]
WFP 215 g/m^2	NFC carboxymethyl	240	31200	
Single layer bio-nanocomposite coating				
KP 120 g/m^2	Chitosan+montmorillonite 5%	2550	-	[185]
BG 70 g/m^2	Chitosan nanosized + NFC10%	0.005	-	[186]
BKP 350 g/m^2	PHB	-	278	[187]
BKP 350 g/m^2	PHB+MFC 1%	-	382	
BKP 350 g/m^2	PHB+MFC 5%	-	610	
BKP 350 g/m^2	PHB+mMFC 1%	-	250	
BKP 350 g/m^2	PHB+mMFC 5%	-	145	
BKP 350 g/m^2	PHB+NFC 1%	-	290	
BKP 350 g/m^2	PHB+NFC 5%	-	210	
*BG 350 g/m^2	Shellac+NFC 2.5%	38.9	275	-
*BG 350 g/m^2	Shellac+mNFC 2.5%	16.4	61	-
Bilayer coating				
BKP 60 g/m^2	Shellac/MFC	6-8	>4000	[188]
KP 191 g/m^2	Resin/NFC-citrate	14886	-	[189]
KP 77.8 g/m^2	Caseinate/chitosan	4285	-	[190]

Note Results from this study, PB: paperboard, LB: linerboard, WFP: wood-free paper, BKP: bleached kraft paper, KP: kraft paper, BG: bagasse paper, WVTR: water vapor transmission rate in g/m^2-day, OTR: oxygen transmission rate in cc/m^2-day.

4.2.4 Oil Resistance

Figure 4.14A shows the oil contact angle (OCA) of uncoated and coated BG sheets. The OCA of the uncoated BG sheet was the lowest (29º) because numerous hydroxyl group on cellulose chains making the BG sheet surface has high surface energy [189]. The shellac coated sample (BG/S) showed an increased OCA to 44º due to the lower surface energy provided by ester groups of shellac [191]. With NFC addition, BG/S-NFC5 showed a decreased OCA (37º) when compared to BG/S. The high surface area of NFC promoted the rich of hydroxyl groups, therefore, increasing surface energy of the coating layer. In the case of BG/S-mNFC5, the OCA increased to 54º which indicated that surface modification of mNFC decreased surface energy of the nanocomposite layer by introducing the ester functional group and led to an increase in oil resistance of the sample. From figure 4.14B, the dynamic oil contact angle (DOCA) on the uncoated BG sheet decreased almost linearly over a short period of time (1 to 11 sec). This result indicated that the high porous BG structure can absorb oil easily [192]. With coating films, the DOCA of all conditions (BG/S, BG/S-NFC5 and BG/S-mNFC5) showed similar trends of lower oil absorption into the sheets. In addition, the photographs in Figure 4.14C compared the oil absorption of the uncoated and coated BG molded pulp samples at room temperature. The results clearly showed that after 30 minutes of holding time, the uncoated BG molded pulp heavily absorbed oil, indicating by the darken area. In contrast, the nanocomposite coated BG molded pulp (BG/S-mNFC5) showed much greater oil resistance with no oil absorption or darken area observed.

Similarly, from the Kit test results in Figure 4.15, the uncoated BG sheet showed evident spots caused by grease penetration and the Kit rating was only 1. On the other hands, the coated BG sheet with nanocomposite demonstrated good greaseproof performance with the Kit rating of 7 since. The kit number of grease-resistant paper used in food packaging should be 5 to 8 [193]. Hence, the nanocomposite based coated BG sheet met the standard of greaser proof food packaging.

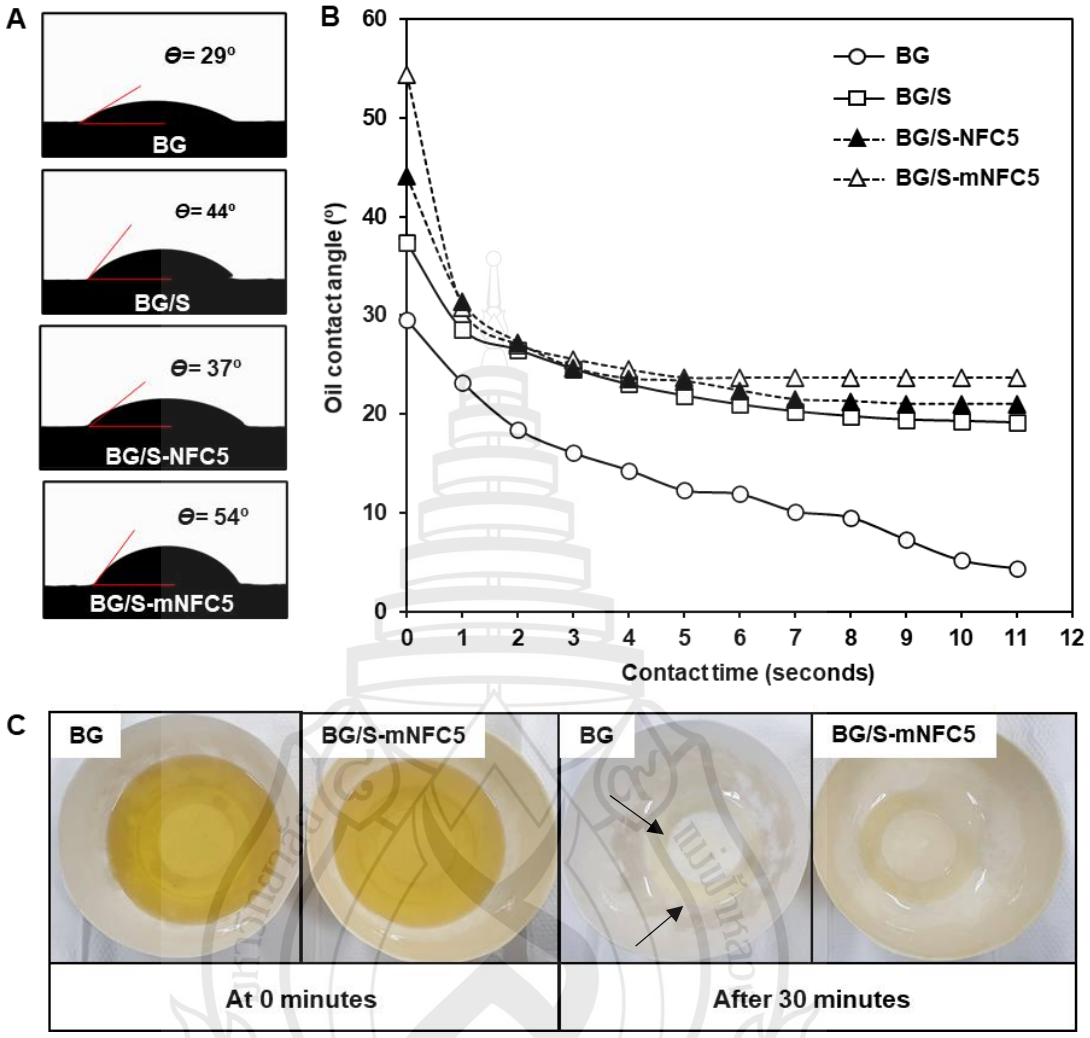

Figure 4.14 (A) Oil Contact Angle (OCA), (B) Dynamic Change in Contact Angle (DCOA) of Oil Drop on Uncoated and Coted BG Sheet. (C) Photograph of Oil Absorption Test in the Uncoated and Coated BG Molded Pulp Before and After 30 Minutes; Black Arrow Indicated Oil Absorbed Area

4.2.5 Thermal Stability

The first step of thermal degradation (Figure 4.16A) of all samples was observed around 100 ºC, which was mainly associated with the evaporation of water due to the hydrophilic character of the fibre and release of residual solvent in shellac [194-195]. Around 250 °C, the first release of acid components (-COOH) from shellac observed

for on the coated BG sheets (BG/S, BG/S-NFC5, and BG/S-mNFC5) [196]. The third step of weight loss at a temperature around 300 °C referred to cellulose degradation [197]. The DTG curves (Figure 4.16B) revealed the temperature for maximum rate of weight loss for all samples is around 364 ºC. The uncoated BG condition showed the highest thermal stability since cellulose has higher thermal degradation than shellac [198]. The last degradation process started at a temperature higher than 450 ºC and ends at about 500 ºC. This presented that large hydrocarbon chains of the shellac were decomposed [199-200].

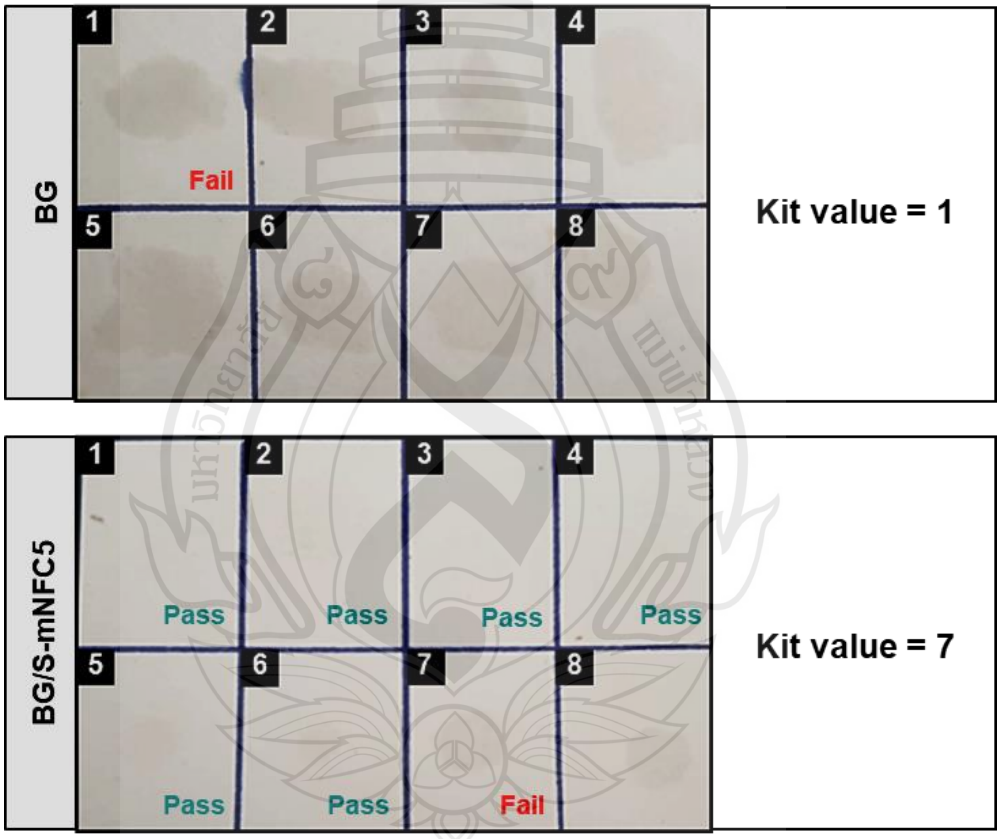

Figure 4.15 Comparison Between the Level of Grease Resistance (Kit Test) of Uncoated and Coated BG Molded Pulp

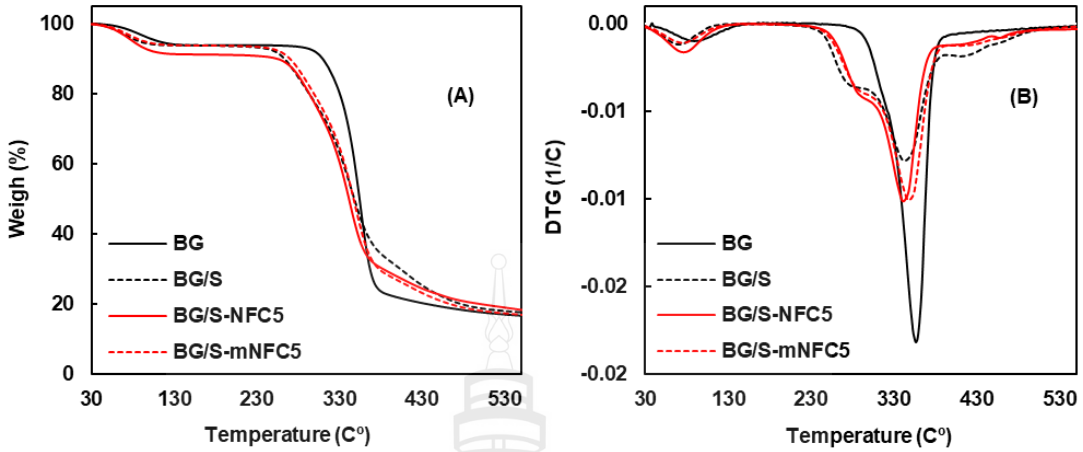

Figure 4.16 (A) Thermogravimetric (TGA) Analysis and; (B) Derivative Thermogravimetric (DTG) Obtained by TGA for the Uncoated BG and Coated BG Sheet Samples

4.2.6 Mechanical Properties

The paper strength was greatly related to the bonding ability between fibres [201-202]. When coating shellac on the BG sheet (BG/S), it significantly ($p<0.01$) increased its UTS, MOE and TI when compared to the pure BG. This indicated the shellac penetration resulted in the highly bonded structure. However, the EAB of BG/S was significantly decreased. The possible reason explained by the brittleness of shellac due to the presence of crosslink [203]. For NFC nanocomposite coating, mechanical properties of BG/S-NFC1 and BG/S-NFC5 were found to decrease with increasing NFC content. The negative effect of poorly dispersed NFC in shellac might make the coating layer lose its homogeneity and lower mechanical properties of the coated sheet [177]. On the other hand, the mechanical properties of BG/S-mNFC1 and BG/S-mNFC5 increased when mNFC loading contents increased. This is probably due to the good dispersion and homogeneity of the coating layer [204-205]. Moreover, the TI of BG/S-mNFC1 and BG/S-mNFC5 were also increased.

Table 4.3 Ultimate Tensile Strength (UTS), Modulus of Elasticity (MOE), Elongation at Break (EAB) and Tensile Index (TI) of Uncoated and Coated BG Sheet

Sample	UTS (MPa)	MOE (GPa)	EAB (%)	TI (Nm/g)
BG (control)	28.32±2.88^{d}	3.07±0.26^{b}	1.67±0.29^{c}	30.10±3.47^{d}
BG/S	38.63±1.19^{a}	3.34±0.32^{a}	1.28±0.24^{f}	41.89±0.90^{a}
BG/S-NFC 1	31.62±5.26^{c}	2.38±0.44^{e}	1.60±0.27^{d}	28.06±4.32^{e}
BG/S-NFC 5	26.04±2.31^{e}	2.86±0.35^{c}	1.45±0.53^{e}	28.35±5.45^{e}
BG/S-mNFC 1	30.17±3.63^{c}	2.54±0.26^{d}	2.04±0.44^{b}	34.41±2.17^{c}
BG/S-mNFC 5	34.75±2.41^{b}	2.87±0.27^{c}	2.53±0.33^{a}	39.13±3.50^{b}

CHAPTER 5

CONCLUSION

In the first part, nanofibrillated cellulose (NFC) was modified by esterification using a sonication-assist method, and characterized using FTIR and ^{13}C NMR to confirm the degree of substitution. It was shown that the sonication amplitude (30%-90%) and time (10-60 min) used for the reaction influenced the degree of ester group substitution on NFC and also the length of oligomeric substituents. High sonication energy led to a partial fragmentation and a decrease in crystallinity of modified NFC or mNFC as revealed by TEM and XRD results. From back-titration, it was found that a lengthy reaction time might also result in a reversed reaction, with damaged NFC and lower DS. When mNFCs were integrated into the BG pulp slurries, the drainage problem during sheet forming as commonly occurs in systems based on NFC was largely solved achieving a similar efficiency as adding retention aid additive (CPAM). After forming the molded sheets, the sheets integrated with mNFCs and NFC+CPAM retained more nanocellulose fibers on their surfaces and internal structures, leading to a denser structure with enhanced mechanical properties. Increased water contact angles were also observed in the mNFC integrated specimens, showing improved surface resistance to water thanks to the substituted ester groups on mNFC. Should be noted that only the sheet integrated with mNFC90 (DS 0.55) demonstrated a significant lower water vapor transmission rate than the other samples, indicating that a sufficient level of the degree of NFC modification by esterification is essential for water vapor barrier properties of the molded pulp products. In the second part, the shellac and nanocomposite were coated on BG surface by solvent casting method. Shellac penetration also improved the strength of BG paper; however, it showed a negative effect on the thermal stability. The nanocomposite of shellac/NFC or mNFC with different loading contents (1-5wt%) showed WVTR and OTR improved 86% and 97%,

respectively compared to the uncoated BG sheet because of good dispersion of mNFC in this system. Figure 5.1 compares barrier properties of common plastic packaging materials and the current coated molded pulps. The OTR and WVTR of the nanocomposite coated samples is in the same range with the plastic-based materials. Moreover, these values suggested that the nanocomposite coated samples could be used instead of LDPE, HDPE, PP, PET, PA6, PVDC, PVC and PS. From the application of food packaging materials shows in Figure 5.2, the current nanocomposite coated molded pulp is now upgraded and can be used for instant food.

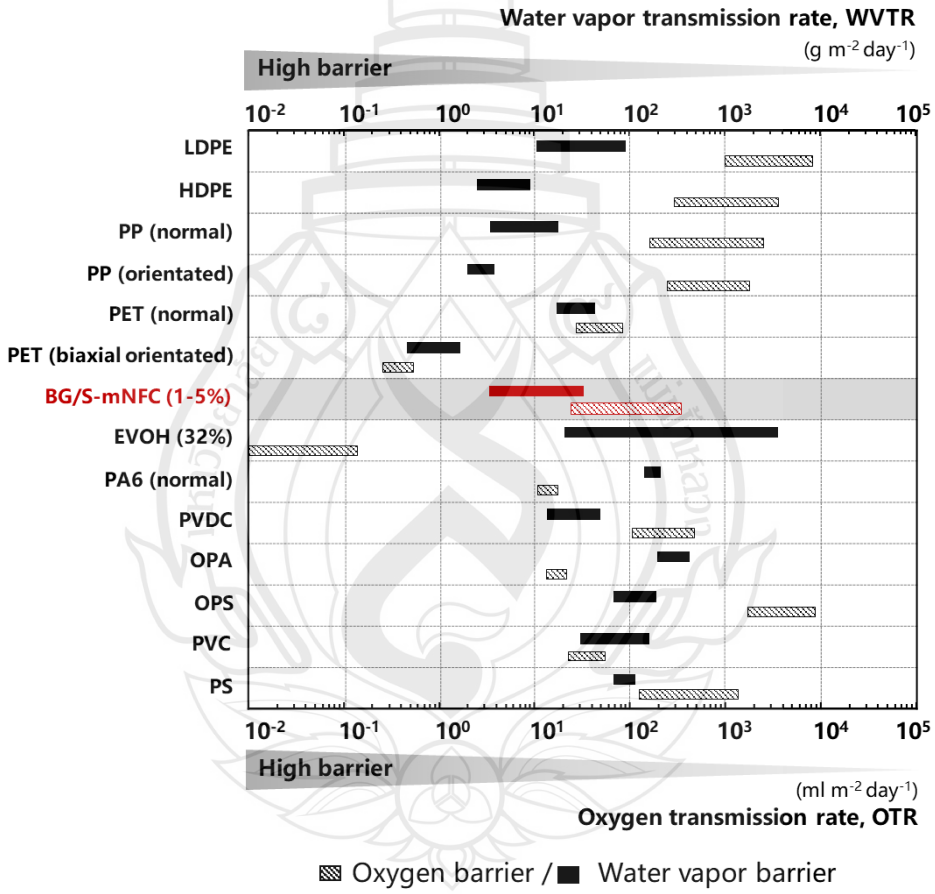

Figure 5.1 Comparison of Permeability Range Between Commercials Selective (Black) and Nanocomposite Materials (Red)

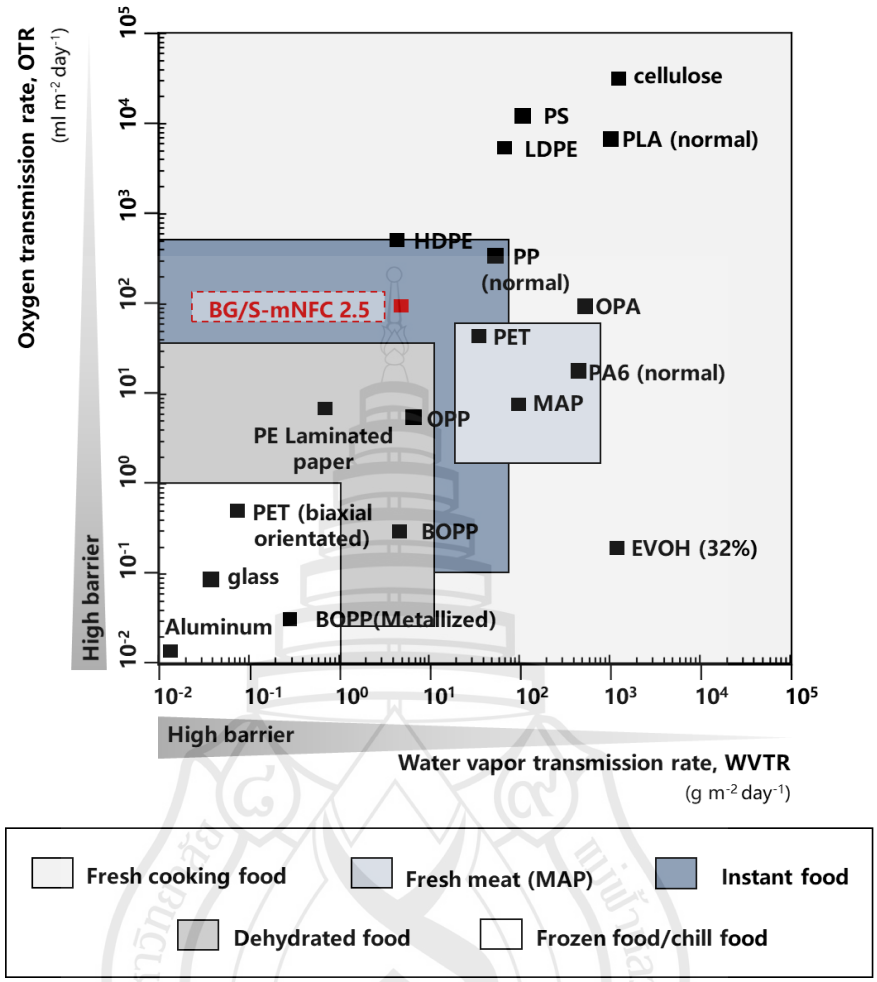

Note LDPE, Low Density Polyethylene; HDPE, High Density Polyethylene; PP, Polypropylene; OPP, Orientated Polypropylene; PET,Polyethylene Terephthalate; S-mNFC (1-5%), Shellac with 1-5% mNFC Based Nanocomposite; EVOH, Ethylene Vinyl Alcohol; PA, Polyamide; PVDC, Polyvinyliden Chloride; OPA, Orientated Polyamide; OPS,Orientated Polystyrene; PVC,Polyvinyl Chloride; PS, Polystyrene.

Figure 5.2 Barrier Requirements of Different Packaging Materials for Various Type of Food

REFERENCES

REFERENCES

[1] Yildirim, S., Röcker, B., Pettersen, M. K., Nilsen-Nygaard, J., . . . Coma, V. (2018). Active packaging applications for food. *Food Science and Food Safety*, *17*(1), 165-199.

[2] Di, J., Reck, B. K., Miatto, A., & Graedel, T. E. (2021). United States plastics: Large flows, short lifetimes, and negligible recycling. *Resources Conservation and Recycling*, *167*, 105440.

[3] Hogarth, C. (2005). 14 Moulded pulp packaging. *Paper and Paperboard Packaging Technology*, 414.

[4] Grönqvist, S., Hakala, T. K., Kamppuri, T., Vehviläinen, M., . . . Suurnäkki, A. (2014). Fibre porosity development of dissolving pulp during mechanical and enzymatic processing. *Cellulose*, *21*(5), 3667-3676.

[5] Lange, J., & Wyser, Y. (2003). Recent innovations in barrier technologies for plastic packaging- a review. *Packaging Technology and Science*, *16*(4), 149-158.

[6] Kim, J. H., Shim, B. S., Kim, H. S., Lee, Y. J., . . . Kim, J. (2015). Review of nanocellulose for sustainable future materials. *International Journal of Precision Engineering and Manufacturing-Green Technology*, *2*(2), 197-213.

[7] Shanmugam, K., Doosthosseini, H., Varanasi, S., Garnier, G., & Batchelor, W. (2019). Nanocellulose films as air and water vapour barriers: A recyclable and biodegradable alternative to polyolefin packaging. *Sustainable Materials and Technologies*, 22, e00115.

[8] Mao, H., Gong, Y., Liu, Y., Wang, S., . . . Wei, C. (2017). Progress in nanocellulose preparation and application. *Paper and Biomaterials*, *2*(4), 65.

[9] Lengowski, E. C., Júnior, E. A. B., Kumode, M. M. N., Carneiro, M. E., & Satyanarayana, K. G. (2019). Nanocellulose in the paper making. *Polymer Composites and Nanocomposites*, 1027-1066.

[10] Nair, S. S., Zhu, J. Y., Deng, Y., & Ragauskas, A. J. (2014). High performance green barriers based on nanocellulose. *Sustainable Chemical Processes*, *2*(1), 1-7.

[11] Tummala, G. K., Joffre, T., Lopes, V. R., Liszka, A., Buznyk, O., Ferraz, N., & Mihranyan, A. (2016). Hyperelastic nanocellulose-reinforced hydrogel of high water content for ophthalmic applications. *ACS Biomaterials Science & Engineering*, *2*(11), 2072-2079.

[12] Cherpinski, A., Torres-Giner, S., Vartiainen, J., Peresin, M. S., . . . Lagaron, J. M. (2018). Improving the water resistance of nanocellulose-based films with polyhydroxyalkanoates processed by the electrospinning coating technique. *Cellulose*, *25*(2), 1291-1307.

[13] Morais, J. P. S., de Freitas Rosa, M., Nascimento, L. D., do Nascimento, D. M., & Cassales, A. R. (2013). Extraction and characterization of nanocellulose structures from raw cotton linter. *Carbohydrate Polymers*, *91*(1), 229-235.

[14] Wang, Y., Wang, X., Xie, Y., & Zhang, K. (2018). Functional nanomaterials through esterification of cellulose: A review of chemistry and application. *Cellulose*, *25*(7), 3703-3731.

[15] Cekota, JA. (2001). *Molded pulp tray*. US: United States patent application 29/111.

[16] Wang, Z. W., & Li, X. F. (2014). Effect of strain rate on cushioning properties of molded pulp products. *Materials & Design*, *57*, 598-607.

[17] Howe, E. (2012). *The re-invention of molded pulp*. NY: Rochester Institute of Technology.

[18] P. Ltd. (2005). *Review of moulded paper pulp*. UK: The Waste & Resources Action Programme.

[19] Dijkstra, W., Kloosterman, H. F., & Niemarkt, C. (2011). *Packaging unit.* US: United States Patent No. 12/996.

[20] Gaikwad, K. K., Singh, S., & Lee, Y. S. (2018). Oxygen scavenging films in food packaging. *Environmental Chemistry Letters*, *16*(2), 523-538.

[21] Berenzon, S., & Saguy, I. S. (1998). Oxygen absorbers for extension of crackers shelf-life. *LWT-Food Science and Technology*, *31*(1), 1-5.

[22] Heinze, T. (2015). Cellulose: Structure and properties. Cellulose chemistry and properties: Fibers. *Nanocelluloses and Advanced Materials, 271*, 1-52.

[23] Broido, A., Javier-Son, A. C., Ouano, A. C., & Barrall, E. M. (1973). Molecular weight decreases in the early pyrolysis of crystalline and amorphous cellulose. *Applied Polymer Science, 17*(12), 3627-3635.

[24] Guiné, R. (2018). The drying of foods and its effect on the physical-chemical, sensorial and nutritional properties. *International Journal of Food Engineering*, *2*(4), 93-100.

[25] Malik, T., & Kajla, P. (2018). Development of ready to cook curry from dried vegetables. *International Journal of Chemical Studies*, 136-140.

[26] Han, J. H. (2005). *Innovations in food packaging*. London UK: Elsevier.

[27] Fu, B. X. (2008). Asian noodles: History, classification, raw materials, and processing. *Food Research International*, *41*(9), 888-902.

[28] Errington, F., Gewertz, D., & Fujikura, T. (2013). *The noodle narratives: The global rise of an industrial food into the twenty-first century*. USA: University of California Press.

[29] Parry, R. T. (2012). *Principles and applications of modified atmosphere packaging of foods*. Manchester: Springer Science & Business Media.

[30] Ling, Q. (2010). *Asian Noodles: Science, Technology and Processing*. US: Packaging of noodle products.

[31] Hanlon, J. F., & Kelsey, R. J. (1998). *Handbook of package engineering*. New York: CRC Press.

[32] Lange, J., & Wyser, Y. (2003). Recent innovations in barrier technologies for plastic packaging-a review. *Packaging Technology and Science, 16*(4), 149-158.

[33] Piergiovanni, L., & Limbo, S. (2016). *Plastic packaging materials*. Basel, Switzerland: Springer.

[34] Cameron, J. M. (2002). *U.S. Patent No. 6,441,117*. Washington, DC: U.S. Patent and Trademark Office.

[35] Raj, B. (2004). Low density polyethylene/starch blend films for food packaging applications. *Advances in Polymer Technology: Journal of the Polymer Processing Institute, 23*(1), 32-45.

[36] Alin, J., & Hakkarainen, M. (2011). Microwave heating causes rapid degradation of antioxidants in polypropylene packaging, leading to greatly increased specific migration to food simulants as shown by ESI-MS and GC-MS. *Journal of Agricultural and Food Chemistry, 59*(10), 5418-5427

[37] Miltz, J., & Rosen-Doody, V. A. R. D. A. (1985). Migration of styrene monomer from polystyrene packaging materials into food simulants. *Journal of Food Processing and Preservation*, *8*(3-4), 151-161.

[38] Bensur, F. J. (2005). *U.S. Patent No. 6,846,532*. Washington, DC: U.S. Patent and Trademark Office.

[39] Anderson, W. E., William, S. R., & Philip, F. C. (1964). *U.S. Patent No. 3,130,647*. Washington, DC: U.S. Patent and Trademark Office.

[40] Schneider, Y., Kluge, C., Weiß, U., & Rohm, H. (2010). *Technology of Cheesemaking*. UK: The society of dairy technology book series.

[41] Coles, R., McDowell, D., & Kirwan, M. J. (Eds.). (2003). Food packaging technology. London UK: CRC press.

[42] Jorgensen, G. J., Terwilliger, K. M., Del Cueto, J. A., Glick, S. H., . . . McMahon, T. J. (2006). Moisture transport, adhesion, and corrosion protection of PV module packaging materials. *Solar Energy Materials and Solar Cells*, *90*(16), 2739-2775.

[43] Krysiak, D. L., Allen, P. E., & Kirihara, T. T. (2004). *U.S. Patent No. 6,746,707.* Washington, DC: U.S. Patent and Trademark Office.

[44] Sorrentino, A., Gorrasi, G., & Vittoria, V. (2007). Potential perspectives of bio-nanocomposites for food packaging applications. *Trends Food Sci. Technol, 18(2)*, 84-95.

[45] Klemm, D., Kramer, F., Moritz, S., Lindström, T., . . . Dorris, A. (2011). Nanocelluloses: A new family of nature-based materials. *Angewandte Chemie International Edition*, *50*(24), 5438–5466.

[46] Abitbol, T., Rivkin, A., Cao, Y., Nevo, Y., . . . Shoseyov, O. (2016). Nanocellulose: A tiny fiber with huge applications. *Biotechnology, 39,* 76-88.

[47] Gousse, C., Chanzy, H., Cerradab, M.L., & Fleury, E. (2004). Surface silylation of cellulose microfibrils: Preparation and rheological properties. *Polymer, 45*(5), 1569-1575.

[48] Hubbe, M. A., Ferrer, A., Tyagi, P., Yin, Y., . . . Rojas, O. J. (2017). Nanocellulose in thin films, coatings, and plies for packaging applications: A review. *Bio Resource, 12*(1), 2143-2233.

[49] Islam, M. T., Alam, M. M., & Zoccola, M. (2013). Review on modification of nanocellulose for application in composites. *Int J Innov Res Sci Eng Technol, 2*(10), 5444-5451.

[50] Kobayashi, S., Uyama, H., Suda, S., & Namekawa, S. (1997). Dehydration polymerization in aqueous medium catalyzed by lipase. *Chem Lett*, 26-105.

[51] Sassi, JF., & Chanzy, H. (1995). Ultrastructural aspects of the acetylation of cellulose. *Cellulose, 2*, 111-127.

[52] Ladouce, L., Fleury, E., Gousse, C., Cantiani, R., . . . Excoffier, G. (2004). *Cellulose microfibrils with modified surface, preparation method and use thereof*. United States patent US 6,703,497. Washington, DC: U.S. Patent and Trademark Office.

[53] Indarti, E., Rohaizu, R., & Wanrosli, W. D. (2019). Silylation of TEMPO oxidized nanocellulose from oil palm empty fruit bunch by 3-aminopropyltriethoxysilane. *International Journal of Biological Macromolecules, 135*, 106-112.

[54] David, G., Gontard, N., Guérin, D., Heux, L., . . . Angellier-Coussy, H. (2019). Exploring the potential of gas-phase esterification to hydrophobize the surface of micrometric cellulose particles. *European Polymer Journal, 115*, 138-146.

[55] Yi, T., Zhao, H., Mo, Q., Pan, D., . . . Song, H. (2020). From cellulose to cellulose nanofibrils-a comprehensive review of the preparation and modification of cellulose nanofibrils. *Materials*, *13*(22), 5062.

[56] Berlioz, S., Molina-Boisseau, S., Nishiyama, Y., & Heux, L. (2009). Gas-phase surface esterification of cellulose microfibrils and whiskers. *Biomacromolecules*, *10*(8), 2144-2151.

[57] Sethi, J., Oksman, K., Illikainen, M., & Sirviö, J. A. (2018). Sonication-assisted surface modification method to expedite the water removal from cellulose nanofibers for use in nanopapers and paper making. *Carbohydrate Polymers*, *197*, 92-99.

[58] Brodin, F. W., Gregersen, Ø. W., & Syverud, K. (2014). Cellulose nanofibrils: Challenges and possibilities as a paper additive or coating material–A review. *Nordic Pulp & Paper Research Journal*, *29*(1), 156-166.

[59] Peydecastaing, J., Girardeau, S., Vaca-Garcia, C., & Borredon, M. E. (2006). Long chain cellulose esters with very low DS obtained with non-acidic catalysts. *Cellulose*, *13*(1), 95-103.

[60] Jonoobi, M., Harun, J., Mathew, A. P., Hussein, M. Z. B., & Oksman, K. (2010). Preparation of cellulose nanofibers with hydrophobic surface characteristics. *Cellulose*, *17*(2), 299-307.

[61] Kim, D. Y., Nishiyama, Y., & Kuga, S. (2002). Surface acetylation of bacterial cellulose. *Cellulose*, *9*(3), 361-367.

[62] Ifuku, S., Nogi, M., Abe, K., Handa, K., . . . Yano, H. (2007). Surface modification of bacterial cellulose nanofibers for property enhancement of optically transparent composites: dependence on acetyl-group DS. *Biomacromolecules*, *8*(6), 1973-1978.

[63] Rodionova, G., Lenes, M., Eriksen, Ø., Hoff, B.H., & Gregersen, Ø.W. (2002). Surface modification of microfibrillated cellulose films by gas-phase esterification. *Improvement of Barrier Properties, 9*, 361-367.

[64] Gousse, C., Chanzy, H., Cerrada, M. L., & Fleury, E. (2004). Surface silylation of cellulose microfibrils: preparation and rheological properties. *Polymer*, *45*(5), 1569-1575.

[65] Missoum, K., Bras, J., & Belgacem, M. N. (2012). Organization of aliphatic chains grafted on nanofibrillated cellulose and influence on final properties. *Cellulose*, *19*(6), 1957-1973.

[66] Nogi, M., Abe, K., Handa, K., Nakatsubo, F., . . . Yano, H. (2006). Property enhancement of optically transparent bionanofiber composites by acetylation. *Applied Physics Letters*, *89*(23), 233123.

[67] Kaplan, D. L. (1998). *Biopolymers from Renewable Resources* (pp.1-29). Berlin: Springer.

[68] Grujić, R., Vujadinović, D., & Savanović, D. (2017). *Biopolymers as food packaging materials* (pp. 139-160). USA: Springer.

[69] Burzic, I., Pretschuh, C., Kaineder, D., Eder, G., . . . Kateryna, W. (2019). Impact modification of PLA using biobased biodegradable PHA biopolymers. *European Polymer Journal*, *114*, 32-38.

[70] Hodzic, A. (2005). *Bacterial polyester-based biocomposites*. USA: CRC Press, 624-643.

[71] Rajan, K. P., Thomas, S. P., Gopanna, A., & Chavali, M. (2019). *Polyhydroxybutyrate (PHB): A standout biopolymer for environmental sustainability* (pp. 2803-2825). USA: Springer.

[72] Mohanty, A. K., Misra, M., & Drzal, L. T. (2005). *Natural fibers, biopolymers, and biocomposites.* USA: CRC press.

[73] Grujic, R., Vukic, M., & Gojkovic, V. (2017). *Advances in Applications of Industrial Biomaterials* (pp. 103-119). Midtown Manhattan: Springer.

[74] Tang, X. Z., Kumar, P., Alavi, S., & Sandeep, K. P. (2012). Recent advances in biopolymers and biopolymer-based nanocomposites for food packaging materials. *Critical Reviews in Food Science and Nutrition*, *52*(5), 426-442.

[75] Woods, C. (1994). The nature and treatment of wax and shellac seals. *Journal of the Society of Archivists*, *15*(2), 203-214.

[76] Azouka, A., Huggett, R., & Harrison, A. (1993). The production of shellac and its general and dental uses: A review. *Journal of Oral Rehabilitation*, *20*(4), 393-400.

[77] Cockeram, H. S., & S. A. Levine. (1961). The physical and chemical properties of shellac. *Chemistry*, *12*(6), 316-323.

[78] Tomé, L. C., Pinto, R. J., Trovatti, E., Freire, C. S., Silvestre, A. J., Neto, C. P., & Gandini, A. (2011). Transparent bionanocomposites with improved properties prepared from acetylated bacterial cellulose and poly (lactic acid) through a simple approach. *Green Chemistry*, *13*(2), 419-427.

[79] Banerjee, P. K., Srivastava, B. C., & Kumar, S. (1982). Shellac-solvent interaction parameter. *Polymer*, *23*(8), 1244-1245.

[80] Michael F., Martin C., Brown R., Duguay C., & Taylor, J. (2020). *Shellac now plentiful at rockler*. Retrieved August 2, 2021 from https://www.canadianwoodworking.com/shellac-now-plentiful-rockler

[81] Lee, K. Y., Tammelin, T., Schulfter, K., Kiiskinen, H., . . . Bismarck, A. (2012). High performance cellulose nanocomposites: Comparing the reinforcing ability of bacterial cellulose and nanofibrillated cellulose. *ACS Applied Materials & Interfaces*, *4*(8), 4078-4086.

[82] George, J., & Ishida, H. (2018). A review on the very high nanofiller-content nanocomposites: Their preparation methods and properties with high aspect ratio fillers. *Progress in Polymer Science*, *86*, 1-39.

[83] Ojijo, V., & Ray, S. S. (2013). Processing strategies in bionanocomposites. *Progress in Polymer Science*, *38*(10-11), 1543-1589.

[84] Jamróz, E., Kulawik, P., & Kopel, P. (2019). The effect of nanofillers on the functional properties of biopolymer-based films: A review. *Polymers*, *11*(4), 675.

[85] Fukuzumi, H., Saito, T., & Isogai, A. (2013). Influence of TEMPO-oxidized cellulose nanofibril length on film properties. *Carbohydrate Polymers*, *93*(1), 172-177.

[86] Viana, L. C., Potulski, D. C., Muniz, G. I. B. D., Andrade, A. S. D., & Silva, E. L. D. (2018). Nanofibrillated cellulose as an additive for recycled paper. *Cerne*, *24*, 140-148.

[87] Ferrer, A., Pal, L., & Hubbe, M. (2017). Nanocellulose in packaging: Advances in barrier layer technologies. *Industrial Crops and Products*, *95*, 574-582.

[88] Nair, S. S., Zhu, J. Y., Deng, Y., & Ragauskas, A. J. (2014). High performance green barriers based on nanocellulose. *Sustainable Chemical Processes*, *2*(1), 1-7.

[89] Eriksen, O., Syverud, K., & Gregersen, O. (2008). The Use of Microfibrillated Cellulose Produced from Kraft Pulp as Strength Enhancer in TMP Paper. *Nordic Pulp and Paper Research Journal*, *23*(3), 299-304.

[90] Taipale, T., Osterberg, M., Nykanen, A., Ruokolainen, J., & Laine, J., (2010). Effect of microfibrillated cellulose and fines on the drainage of kraft pulp suspension and paper strength. *Cellulose*, *17*(5), 1005-1020.

[91] Manninen, M., Kajanto, I., Happonen, J., & Paltakari, J., (2011). The Effect of microfibrillated cellulose addition on drying shrinkage and dimensional stability of wood-free paper. *Nordic Pulp and Paper Research Journal*, *26*(3), 297-305.

[92] Hejnesson-Hultén, A., Basta, J., Samuelsson, M., Greschik, T., . . . Daniel, G. (2012). The influence of microfibrillated cellulose (MFC) on paper strength and surface properties. *Bioresources*, *7*(3), 3051.

[93] Kajanto, I., & Kosonen, M. (2012). The potential use of micro-and nanofibrillated cellulose as a reinforcing element in paper. *Journal of Science & Technology for Forest Products and Processes*, *2*(6), 42-48.

[94] Sethi, J., Oksman, K., Illikainen, M., & Sirviö, J. A. (2018). Sonication-assisted surface modification method to expedite the water removal from cellulose nanofibers for use in nanopapers and paper making. *Carbohydrate Polymers*, *197*, 92-99.

[95] Lu, J., Askeland, P., & Drzal, L. T. (2008). Surface modification of microfibrillated cellulose for epoxy composite applications. *Polymer*, *49*(5), 1285-1296.

[96] Bras, J., Hassan, M. L., Bruzesse, C., Hassan, E. A., . . . Dufresne, A. (2010). Mechanical, barrier, and biodegradability properties of bagasse cellulose whiskers reinforced natural rubber nanocomposites. *Industrial Crops and Products*, *32*(3), 627-633.

[97] Saha, N. R., Sarkar, G., Roy, I., Bhattacharyya, A., . . . Chattopadhyay, D. (2016). Nanocomposite films based on cellulose acetate/polyethylene glycol/modified montmorillonite as nontoxic active packaging material. *RSC Advances*, *6*(95), 92569-92578.

[98] Fernandes, S. C., Freire, C. S., Silvestre, A. J., Pascoal Neto, C., & Gandini, A. (2011). Novel materials based on chitosan and cellulose. *Polymer International*, *60*(6), 875-882.

[99] Kritchenkov, A. S., Egorov, A. R., Volkova, O. V., Artemjev, A. A., . . . Khrustalev, V. N. (2021). Novel biopolymer-based nanocomposite food coatings that exhibit active and smart properties due to a single type of nanoparticles. *Food Chemistry*, *343*, 128676.

[100] Wu, Z., Deng, W., Luo, J., & Deng, D. (2019). Multifunctional nano-cellulose composite films with grape seed extracts and immobilized silver nanoparticles. *Carbohydrate Polymers*, *205*, 447-455.

[101] Herrera, M. A., Sirviö, J. A., Mathew, A. P., & Oksman, K. (2016). Environmentally friendly and sustainable gas barrier on porous materials: Nanocellulose coatings prepared using spin-and dip-coating. *Materials & Design*, *93*, 19-25.

[102] Mondragon, G., Peña-Rodriguez, C., González, A., Eceiza, A., & Arbelaiz, A. (2015). Bionanocomposites based on gelatin matrix and nanocellulose. *European Polymer Journal*, *62*, 1-9.

[103] Song, Z., Xiao, H., & Zhao, Y. (2014). Hydrophobic-modified nano-cellulose fiber/PLA biodegradable composites for lowering water vapor transmission rate (WVTR) of paper. *Carbohydrate Polymers*, *111*, 442-448.

[104] Shankar, G. M., Li, S., Mehta, T. H., Garcia-Munoz, A., . . . Selkoe, D. J. (2008). Amyloid-β protein dimers isolated directly from Alzheimer's brains impair synaptic plasticity and memory. *Nature medicine*, *14*(8), 837-842.

[105] Zahedi, M. T., Tabarsa, M., Madhoushi, & Shakeri, A. R. (2013). Effect of nanoclay (Montmorillonite) on the physical-mechanical properties of polypropylene/wood flour composites, *20*(3), 95-110.

[106] Cui, S., Liu, Y., Fan, M. H., Cooper, A. T., . . . Shen, X. D. (2011). Temperature dependent microstructure of MTES modified hydrophobic silica aerogels. *Materials Letters*, *65*(4), 606-609.

[107] Weththimuni, M. L., Capsoni, D., Malagodi, M., Milanese, C., & Licchelli, M. (2016). Shellac/nanoparticles dispersions as protective materials for wood. *Applied Physics A*, *122*(12), 1-12.

[108] Dhar, P., Bhardwaj, U., Kumar, A., & Katiyar, V. (2015). Poly (3-hydroxybutyrate)/ cellulose nanocrystal films for food packaging applications: Barrier and migration studies. *Polymer Engineering & Science*, *55*(10), 2388-2395.

[109] Song, Z., Xiao, H., & Zhao, Y. (2014). Hydrophobic-modified nano-cellulose fiber/PLA biodegradable composites for lowering water vapor transmission rate (WVTR) of paper. *Carbohydrate Polymers*, *111*, 442-448.

[110] Yang, W., Fortunati, E., Dominici, F., Giovanale, G., . . . Puglia, D. (2016). Synergic effect of cellulose and lignin nanostructures in PLA based systems for food antibacterial packaging. *European Polymer Journal*, *79*, 1-12.

[111] Salehudin, M. H., Salleh, E., Mamat, S. N. H., & Muhamad, I. I. (2014). Starch based active packaging film reinforced with empty fruit bunch (EFB) cellulose nanofiber. *Procedia Chemistry*, *9*, 23-33.

[112] Fernandes, S. C., Oliveira, L., Freire, C. S., Silvestre, A. J., . . . Desbriéres, J. (2009). Novel transparent nanocomposite films based on chitosan and bacterial cellulose. *Green Chemistry*, *11*(12), 2023-2029.

[113] Yang, S., Tang, Y., Wang, J., Kong, F., & Zhang, J. (2014). Surface treatment of cellulosic paper with starch-based composites reinforced with nanocrystalline cellulose. *Industrial & Engineering Chemistry Research*, *53*(36), 13980-13988.

[114] Zhou, J. J., Wang, S. Y., & Gunasekaran, S. (2009). Preparation and characterization of whey protein film incorporated with TiO_2 nanoparticles. *Journal of Food Science*, *74*(7), 50-56.

[115] Jafari, H., Pirouzifard, M., Khaledabad, M. A., & Almasi, H. (2016). Effect of chitin nanofiber on the morphological and physical properties of chitosan/silver nanoparticle bionanocomposite films. *International Journal of Biological Macromolecules*, *92*, 461-466.

[116] Farahnaky, A., Dadfar, S. M. M., & Shahbazi, M. (2014). Physical and mechanical properties of gelatin-clay nanocomposite. *Journal of Food Engineering*, *122*, 78-83.

[117] Nafchi, A. M., Nassiri, R., Sheibani, S., Ariffin, F., & Karim, A. A. (2013). Preparation and characterization of bionanocomposite films filled with nanorod-rich zinc oxide. *Carbohydrate Polymers*, *96*(1), 233-239.

[118] Song, Z., Xiao, H., & Zhao, Y. (2014). Hydrophobic-modified nano-cellulose fiber/PLA biodegradable composites for lowering water vapor transmission rate (WVTR) of paper. *Carbohydrate Polymers*, *111*, 442-448.

[119] Weththimuni, M. L., Capsoni, D., Malagodi, M., Milanese, C., & Licchelli, M. (2016). Shellac/nanoparticles dispersions as protective materials for wood. *Applied Physics A*, *122*(12), 1-12.

[120] Shojaeiarani, J., Bajwa, D., & Holt, G. (2020). Sonication amplitude and processing time influence the cellulose nanocrystals morphology and dispersion. *Nanocomposites*, *6*(1), 41-46.

[121] Sethi, J., Farooq, M., Sain, S., Sain, M., . . . Oksman, K. (2018). Water resistant nanopapers prepared by lactic acid modified cellulose nanofibers. *Cellulose*, *25*(1), 259-268.

[122] Stöllman, U., Johansson, F., & Leufven, A. (1994). Packaging and food quality. *Shelf life evaluation of foods*. Boston: Springer, 52-71.

[123] Fabra, M. J., López-Rubio, A., Ambrosio-Martín, J., & Lagaron, J. M. (2016). Improving the barrier properties of thermoplastic corn starch-based films containing bacterial cellulose nanowhiskers by means of PHA electrospun coatings of interest in food packaging. *Food Hydrocolloids*, *61*, 261-268.

[124] Almasi, H., Ghanbarzadeh, B., Dehghannya, J., Entezami, A. A., & Asl, A. K. (2015). Novel nanocomposites based on fatty acid modified cellulose nanofibers/poly (lactic acid): Morphological and physical properties. *Food Packaging and Shelf Life*, *5*, 21-31.

[125] Peydecastaing, J., Girardeau, S., Vaca-Garcia, C., & Borredon, M. E. (2006). Long chain cellulose esters with very low DS obtained with non-acidic catalysts. *Cellulose*, *13*(1), 95-103.

[126] Atalla, R. H., Gast, J. C., Sindorf, D. W., Bartuska, V. J., & Maciel, G. E. (1980). Carbon-13 NMR spectra of cellulose polymorphs. *Journal of the American Chemical Society*, *102*(9), 3249-3251.

[127] Singh, M., Kaushik, A., & Ahuja, D. (2016). Surface functionalization of nanofibrillated cellulose extracted from wheat straw: Effect of process parameters. *Carbohydrate Polymers, 150*, 48-56.

[128] Tajvidi, M., & Bousfield, D. (2020). Based Oil Barrier Packaging using Lignin-Containing Cellulose Nanofibrils. *Molecules*, *25*(6),1344.

[129] Khonsari, Y. N., Mirshokraei, S. A., & Abdolkhani, A. (2013). Dissolution of wood flour and lignin in 1-butyl-3-methyl-1-imidazolium chloride. *Oriental Journal of Chemistry*, *29*(3), 889.

[130] Śliwiński, A. (1990). Acousto-optics and its perspectives in research and applications. *Ultrasonics*, *28*(4), 195-213.

[131] Xiong, L., & Yu, W. D. (2013). Analysis of the cellulose macromolecule structure after acid treatment by FTIR microspectroscopy. *J. Cellulose Sci. Technol*, *2*, 59-62.

[132] Hu, Z., Zhai, R., Li, J., Zhang, Y., & Lin, J. (2017). Preparation and characterization of nanofibrillated cellulose from bamboo fiber via ultrasonication assisted by repulsive effect. *International Journal of Polymer Science*, 2017.

[133] Zhang, K., Brendler, E., Geissler, A., & Fischer, S. (2011). Synthesis and spectroscopic analysis of cellulose sulfates with regulable total degrees of substitution and sulfation patterns via 13C NMR and FT Raman spectroscopy. *Polymer*, *52*(1), 26-32.

[134] Berlioz, S., Molina-Boisseau, S., Nishiyama, Y., & Heux, L. (2009). Gas-phase surface esterification of cellulose microfibrils and whiskers. *Biomacromolecules*, *10*(8), 2144-2151.

[135] Ramírez, J. A. Á., Suriano, C. J., Cerrutti, P., & Foresti, M. L. (2014). Surface esterification of cellulose nanofibers by a simple organocatalytic methodology. *Carbohydrate Polymers*, *114*, 416-423.

[136] Mason, T. J., & Lorimer, J. P. (1981). *Ultrasound: theory, applications and uses of ultrasound in chemistry*. Chichester: Ellis Horwood Ltd.

[137] Wang, Y., Wang, X., Xie, Y., & Zhang, K. (2018). Functional nanomaterials through esterification of cellulose: A review of chemistry and application. *Cellulose*, *25*(7), 3703-3731.

[138] Eyley, S., & Thielemans, W. (2014). Surface modification of cellulose nanocrystals. *Nanoscale*, *6*(14), 7764-7779.

[139] Rowland, S. P., & Howley, P. S. (1988). Hydrogen bonding on accessible surfaces of cellulose from various sources and relationship to order within crystalline regions. *Polymer Chemistry*, *26*(7), 1769-1778.

[140] Wertz, J. L., Bedue, O., & Mercier, J. P. (2010). *Structure and properties of cellulose* (pp.87-146). Lausanne: EPFL Press.

[141] Olah, G. A., Reddy, V. P., Rasul, G., & Surya Prakash, G. K. (1999). Search for Long-Lived 1, 3-Carbodications and Preparation of the Persistent 1, 1, 3, 3-Tetracyclopropyl-1, 3-propanediyl Dication1. *Journal of the American Chemical Society*, *121*(43), 9994-9998.

[142] Chen, W., Yu, H., Liu, Y., Chen, P., . . . Hai, Y. (2011). Individualization of cellulose nanofibers from wood using high-intensity ultrasonication combined with chemical pretreatments. *Carbohydrate Polymers*, *83*(4), 1804-1811.

[143] Babicka, M., Woźniak, M., Dwiecki, K., Borysiak, S., & Ratajczak, I. (2020). Preparation of nanocellulose using ionic liquids: 1-propyl-3-methylimidazolium chloride and 1-ethyl-3-methylimidazolium chloride. *Molecules, 25*(7), 1544.

[144] Hassanzadeh, M., Sabo, R., Rudie, A., Reiner, R., . . . Oporto, G. S. (2017). Nanofibrillated cellulose from Appalachian hardwoods logging residues as template for antimicrobial copper. *Journal of Nanomaterials*, *2017*, 1-14.

[145] Taipale, T., Österberg, M., Nykänen, A., Ruokolainen, J., & Laine, J. (2010). Effect of microfibrillated cellulose and fines on the drainage of kraft pulp suspension and paper strength. *Cellulose*, *17*(5), 1005-1020.

[146] Österberg, M., & Cranston, E. D. (2014). Special issue on nanocellulose. *Nordic Pulp & Paper Research Journal*, *29*(1), 4-5.

[147] La Mantia, F. P., & Morreale, M. (2011). Green composites: A brief review. *Composites Part A: Applied Science and Manufacturing*, *42*(6), 579-588.

[148] Vajihinejad, V., Gumfekar, S. P., Bazoubandi, B., Rostami Najafabadi, Z., & Soares, J. B. (2019). Water soluble polymer flocculants: Synthesis, characterization, and performance assessment. *Macromolecular Materials and Engineering*, *304*(2), 1800526.

[149] Didone, M., Saxena, P., Brilhuis-Meijer, E., Tosello, G., . . . Howard, T. J. (2017). Moulded pulp manufacturing: overview and prospects for the process technology. *Packaging Technology and Science*, *30*(6), 231-249.

[150] Yu, T., Ren, J., Li, S., Yuan, H., & Li, Y. (2010). Effect of fiber surface-treatments on the properties of poly (lactic acid)/ramie composites. *Composites Part A: Applied Science and Manufacturing*, *41*(4), 499-505.

[151] Khalil, H. A., Davoudpour, Y., Islam, M. N., Mustapha, A., . . . Jawaid, M. (2014). Production and modification of nanofibrillated cellulose using various mechanical processes: A review. *Carbohydrate Polymers*, 99, 649-665.

[152] Petroudy, S. R. D., Sheikhi, P., & Ghobadifar, P. (2017). Sugarcane bagasse paper reinforced by cellulose nanofiber (CNF) and bleached softwood kraft (BSWK) pulp. *Journal of Polymers and the Environment*, *25*(2), 203-213.

[153] Rantanen, J., & Maloney, T. C. (2015). Consolidation and dewatering of a microfibrillated cellulose fiber composite paper in wet pressing. *European Polymer Journal*, *68*, 585-591.

[154] Van Voorn, B., Smit, H. H. G., Sinke, R. J., & De Klerk, B. (2001). Natural fibre reinforced sheet moulding compound. *Composites Part A: Applied Science and Manufacturing*, *32*(9), 1271-1279.

[155] Mao, R., Goutianos, S., Tu, W., Meng, N., . . . Peijs, T. (2017). Comparison of fracture properties of cellulose nanopaper, printing paper and buckypaper. *Journal of Materials Science*, *52*(16), 9508-9519.

[156] Mao, R., Meng, N., Tu, W., & Peijs, T. (2017). Toughening mechanisms in cellulose nanopaper: the contribution of amorphous regions. *Cellulose*, *24*(11), 4627-4639.

[157] Brodin, F. W., Gregersen, Ø. W., & Syverud, K. (2014). Cellulose nanofibrils: Challenges and possibilities as a paper additive or coating material–A review. *Nordic Pulp & Paper Research Journal*, *29*(1), 156-166.

[158] Sallih, N., Lescher, P., & Bhattacharyya, D. (2014). Factorial study of material and process parameters on the mechanical properties of extruded kenaf fibre/polypropylene composite sheets. *Composites Part A: Applied Science and Manufacturing*, 61, 91-107.

[159] Goutianos, S., Mao, R., & Peijs, T. (2018). Effect of inter-fibre bonding on the fracture of fibrous networks with strong interactions. *International Journal of Solids and Structures*, 136, 271-278.

[160] Raj, P., Varanasi, S., Batchelor, W., & Garnier, G. (2015). Effect of cationic polyacrylamide on the processing and properties of nanocellulose films. *Journal of Colloid and Interface Science*, *447*, 113-119.

[161] Zhou, J., Liu, F., & Pan, C. (2014). Effects of cationic polyacrylamide characteristics on sewage sludge dewatering and moisture evaporation. *PloS one*, *9*(5), e98159.

[162] Liu, Y., Zheng, H., Wang, Y., Zheng, X., . . . Zhao, C. (2018). Synthesis of a cationic polyacrylamide by a photocatalytic surface-initiated method and evaluation of its flocculation and dewatering performance: Nano-TiO 2 as a photo initiator. *RSC Advances*, *8*(50), 28329-28340.

[163] Gupta, S., John, A., & Kumar, V. S. (2016). Studies on effect of coat thickness on the moisture uptake by a hardwood substrate. *Maderas. Ciencia y Tecnología*, *18*(3), 443-456.

[164] Lavoine, N., Desloges, I., Khelifi, B., & Bras, J. (2014). Impact of different coating processes of microfibrillated cellulose on the mechanical and barrier properties of paper. *Journal of Materials Science*, *49*(7), 2879-2893.

[165] Mirmehdi, S., de Oliveira, M. L. C., Hein, P. R. G., Dias, M. V., . . . Tonoli, G. H. D. (2018). Spraying cellulose nanofibrils for improvement of tensile and barrier properties of writing & printing (W&P) paper. *Journal of Wood Chemistry and Technology*, *38*(3), 233-245.

[166] Han, J. H., & Krochta, J. M. (1999). Wetting properties and water vapor permeability of whey-protein-coated paper. *Transactions of the ASAE*, *42*(5), 1375.

[167] Wang, J., Chen, L., & He, Y. (2008). Preparation of environmentally friendly coatings based on natural shellac modified by diamine and its applications for copper protection. *Progress in Organic Coatings*, *62*(3), 307-312.

[168] Nair, S. S., Zhu, J. Y., Deng, Y., & Ragauskas, A. J. (2014). High performance green barriers based on nanocellulose. *Chemical Processes*, *2*(1), 1-7.

[169] Weththimuni, M. L., Capsoni, D., Malagodi, M., Milanese, C., & Licchelli, M. (2016). Shellac/nanoparticles dispersions as protective materials forwood. *Applied Physics A*, *122*(12), 1-12.

[170] Yook, S., Park, H., Park, H., Lee, S. Y., . . . Youn, H. J. (2020). Barrier coatings with various types of cellulose nanofibrils and their barrier properties. *Cellulose*, *27*(8), 4509-4523.

[171] Tomadakis, M. M., & Sotirchos, S. V. (1993). Ordinary and transition regime diffusion in random fiber structures. *AIChE Journal*, *39*(3), 397-412.

[172] Cui, Y., Kundalwal, S. I., & Kumar, S. (2016). Gas barrier performance of graphene/polymer nanocomposites. *Carbon*, 98, 313-333.

[173] Cervin, N. T., Aulin, C., Larsson, P. T., & Wågberg, L. (2012). Ultra-porous nanocellulose aerogels as separation medium for mixtures of oil/water liquids. *Cellulose*, *19*(2), 401-410.

[174] Willberg-Keyriläinen, P., Vartiainen, J., Pelto, J., & Ropponen, J. (2017). Hydrophobization and smoothing of cellulose nanofibril films by cellulose ester coatings. *Carbohydrate Polymers*, *170*, 160-165.

[175] Tuil, R. V., Schennink, G., Beukelaer, H. D., Heemst, J. V., & Jaeger, R. (2000). Converting biobased polymers into food packagings. In *The Food Biopack Conference, Copenhagen (Denmark), 27-29 Aug 2000*. KVL.

[176] Okubayashi, S., Griesser, U. J., & Bechtold, T. (2004). A kinetic study of moisture sorption and desorption on lyocell fibers. *Carbohydrate Polymers*, *58*(3), 293-299.

[177] Du, Y., Wang, L., Mu, R., Wang, Y., . . . Pang, J. (2019). Fabrication of novel Konjac glucomannan/shellac film with advanced functions for food packaging. *International Journal of Biological Macromolecules*, 131, 36-42.

[178] Belbekhouche, S., Bras, J., Siqueira, G., Chappey, C., . . . Dufresne, A. (2011). Water sorption behavior and gas barrier properties of cellulose whiskers and microfibrils films. *Carbohydrate Polymers*, *83*(4), 1740-1748.

[179] Lavoine, N., Desloges, I., Khelifi, B., & Bras, J. (2014). Impact of different coating processes of microfibrillated cellulose on the mechanical and barrier properties of paper. *Journal of Materials Science*, *49*(7), 2879-2893.

[180] Littunen, K., Hippi, U., Saarinen, T., & Seppälä, J. (2013). Network formation of nanofibrillated cellulose in solution blended poly (methyl methacrylate) composites. *Carbohydrate Polymers*, *91*(1), 183-190.

[181] Tomadakis, M. M., & Sotirchos, S. V. (1993). Ordinary and transition regime diffusion in random fiber structures. *AIChE Journal*, *39*(3), 397-412.

[182] Kumar, V., Elfving, A., Koivula, H., Bousfield, D., & Toivakka, M. (2016). Roll-to-roll processed cellulose nanofiber coatings. *Industrial & Engineering Chemistry Research*, *55*(12), 3603-3613.

[183] Yook, S., Park, H., Park, H., Lee, S. Y., . . . Youn, H. J. (2020). Barrier coatings with various types of cellulose nanofibrils and their barrier properties. *Cellulose*, *27*(8), 4509-4523.

[184] Hult, E. L., Iotti, M., & Lenes, M. (2010). Efficient approach to high barrier packaging using microfibrillar cellulose and shellac. *Cellulose*, *17*(3), 575-586.

[185] Hassan, E. A., Hassan, M. L., Abou-Zeid, R. E., & El-Wakil, N. A. (2016). Novel nanofibrillated cellulose/chitosan nanoparticles nanocomposites films and their use for paper coating. *Industrial Crops and Products*, *93*, 219-226.

[186] Bhushan, B. (2019). Bioinspired oil–water separation approaches for oil spill clean-up and water purification. *Philosophical Transactions of the Royal Society A*, *377*(2150), 20190120.

[187] Wang, S., & Jing, Y. (2017). Effects of formation and penetration properties of biodegradable montmorillonite/chitosan nanocomposite film on the barrier of package paper. *Applied Clay Science*, 138, 74-80.

[188] Aulin, C., & Ström, G. (2013). Multilayered alkyd resin/nanocellulose coatings for use in renewable packaging solutions with a high level of moisture resistance. *Industrial & Engineering Chemistry Research*, *52*(7), 2582-2589.

[189] Rastogi, V. K., & Samyn, P. (2020). Compression Molding of Polyhydroxybutyrate Nano-composite Films as Coating on Paper Substrates. *Materials Proceedings*, *2*(1), 31.

[190] Khwaldia, K., Basta, A. H., Aloui, H., & El-Saied, H. (2014). Chitosan–caseinate bilayer coatings for paper packaging materials. *Carbohydrate Polymers*, 99, 508-516.

[191] Kraisit, P., Limmatvapirat, S., Nunthanid, J., Luangtana-Anan, M., . . . Yoshihashi, Y. (2012). Determination of Surface Free Energy and Contact Angle for Hydrolyzed Shellac. *Advanced Materials Research*, *506*, 270-273.

[192] Rhim, J. W., Lee, J. H., & Hong, S. I. (2006). Water resistance and mechanical properties of biopolymer (alginate and soy protein) coated paperboards. *LWT-Food Science and Technology*, *39*(7), 806-813.

[193] Xie, J., Xu, J., Cheng, Z., Chen, J., . . . Sheng, J. (2020). Facile synthesis of fluorine-free cellulosic paper with excellent oil and grease resistance. *Cellulose*, *27*, 7009-7022.

[194] Souza, A. G. D., Kano, F. S., Bonvent, J. J., & Rosa, D. D. S. (2017). Cellulose nanostructures obtained from waste paper industry: A comparison of acid and mechanical isolation methods. *Materials Research*, *20*, 209-214.

[195] He, Z., Wang, Z., Zhao, Z., Yi, S., . . . Wang, X. (2017). Influence of ultrasound pretreatment on wood physiochemical structure. *Ultrasonics Sonochemistry*, *34*, 136-141.

[196] Liu, M., Xu, G., Wang, J., Tu, X., . . . Xu, W. (2020). Effects of Shellac Treatment on Wood Hygroscopicity, Dimensional Stability and Thermostability. *Coatings*, *10*(9), 881.

[197] Gagić, T., Perva-Uzunalić, A., Knez, Z., & Škerget, M. (2018). Hydrothermal degradation of cellulose at temperature from 200 to 300 C. *Industrial & Engineering Chemistry Research*, *57*(18), 6576-6584.

[198] Mohomane, S. M., Motaung, T. E., & Revaprasadu, N. (2017). Thermal degradation kinetics of sugarcane bagasse and soft wood cellulose. *Materials*, *10*(11), 1246.

[199] Silakhori, M., Naghavi, M. S., Metselaar, H. S. C., Mahlia, T. M. I., . . . Mehrali, M. (2013). Accelerated thermal cycling test of microencapsulated paraffin wax/polyaniline made by simple preparation method for solar thermal energy storage. *Materials*, *6*(5), 1608-1620.

[200] Han, J. H., & Krochta, J. M. (2001). Physical properties and oil absorption of whey-protein-coated paper. *Journal of Food Science*, *66*(2), 294-299.

[201] Kim, J. H., Nizami, A., Hwangbo, Y., Jang, B., . . . Kim, T. S. (2013). Tensile testing of ultra-thin films on water surface. *Nature Communications*, *4*(1), 1-6.

[202] Han, J. H., & Krochta, J. M. (2001). Physical properties and oil absorption of whey-protein-coated paper. *Journal of Food Science*, *66*(2), 294-299.

[203] Azeredo, H. M., Mattoso, L. H. C., Avena-Bustillos, R. J., Filho, G. C., . . . McHugh, T. H. (2010). Nanocellulose reinforced chitosan composite films as affected by nanofiller loading and plasticizer content. *Journal of Food Science*, *75*(1), N1-N7.

[204] Liu, M., Wang, Z., Liu, P., Wang, Z., . . . Yao, X. (2019). Supramolecular silicone coating capable of strong substrate bonding, readily damage healing, and easy oil sliding. *Science Advances*, *5*(11), eaaw5643.

[205] Arbatan, T., Zhang, L., Fang, X. Y., & Shen, W. (2012). Cellulose nanofibers as binder for fabrication of superhydrophobic paper. *Chemical Engineering Journal*, *210*, 74-79.

CURRICULUM VITAE

CURRICULUM VITAE

NAME Miss Supattra Klayya

DATE OF BIRTH 29 September 1995

ADDRESS No. 56 Moo3 Surasak
Sriracha, Chonburi, Thailand
20110

EDUCATIONAL BACKGROUND

2018 Bachelor of Science
Applied Chemistry
Mae Fah Luang University, Thailand

WORK EXPERIENCE

2018-2021 Teaching Assistant in Statistic and Experimental Design, Mathematics for Life and Science and Mathematics all Around

2021 Project Development of Fully Sustainable Packaging Toward High Performance and High Barrier Properties with SCG Packaging Company

2021-2022 Researcher at Queen Mary University of London (QMUL).

PUBLICATIONS

Punyamoonwongsa, P., Klayya, S., Sajomsang, W., Kunyanee, C., & Aueviriyavit, S. (2019). Silk sericin semi-interpenetrating network hydrogels based on PEG-diacrylate for wound healing treatment. *Polymer Science, 2019*.

Klayya, S., Rattanawongkun, P., Kunfong, N., Yodsuwan, N., Tawichai, N., Intatha, U., & Soykeabkaew, N. (2019). Bagasse sheets reinforced with nanofibrillated celluloses. *Materials Science and Engineering*, *559*(1), 012005.

Soykeabkaew, N., Rattanawongkun, P., Kunfong, N., Klayya, S., Tawichai, N., & Intatha, U. Micro/nanostructured papers from bagasse pulp reinforced by nanofibrillated cellulose from different agro-waste sources. *Advanced Materials Letters*, *10*(11), 814-818.

Rattanawongkun, P., Kunfong, N., Klayya, S., Chotimarnon, T., Duangphet, S., Tawichai, N., & Soykeabkaew, N. (2020). Comparison of molded pulps from rice straw, pineapple leaf and banana stem pulps. *Science Asia*, *46*, 79-84.

Klayya, S., Chotimarnon, T., Tawichai, N., Intatha, U., & Soykeabkaew, N. (2021). Effect of mono-and bilayer coating of nanofibrillated cellulose, its modification, and shellac on properties of molded pulps. *Key Engineering Materials*, *889*, 79-84.

Klayya, S., Tawichai, N., Intatha, U., Zhang, H., Bilotti, E., & Soykeabkaew, N. (2021). Tailoring nanofibrillated cellulose through sonication and its potential use in molded pulp packaging. *Nanocomposites*, *7*(1), 109-122.